NWC TP 5881

12 B.S.

Evaluation of the Harpoon Missile Shock Environment During Ejection Launch by Aircraft Launchers

by
Allan G. Piersol
Bolt Baranek and Newman Inc.
for the
Engineering Department

FEBRUARY 1977

Naval Weapons Center
CHINA LAKE, CALIFORNIA 93555

Naval Weapons Center

AN ACTIVITY OF THE NAVAL MATERIAL COMMAND

R. G. Freeman, III, RAdm., USN ..... Commander
G. L. Hollingsworth ..... Technical Director

FOREWORD

The tests described in this report were performed from July 1973 to November 1975 under AIRTASK AO5P-204/2162/6000/00000 and Work Unit A-05P-204A/RGM-84-S. It is a final report that analyzes the shock spectra environment of a Harpoon missile at ejection.

This report is released at the working level. Because of the continuing nature of this effort, it is probable that further testing will be conducted.

This report was reviewed for technical accuracy by W. N. Jones.

Released by
B. W. HAYS, *Head*
Engineering Department
7 January 1976

Under authority of
G. L. HOLLINGSWORTH
Technical Director

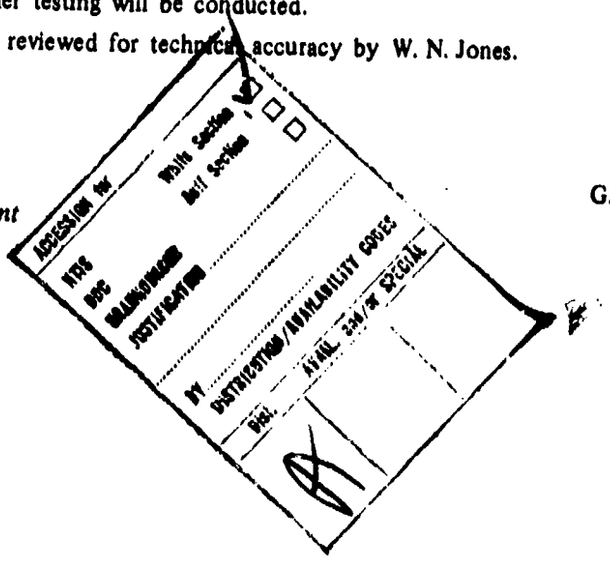

NWC Technical Publication 5881

Published by ..... Technical Information Department
Collation ..... Cover, 20 leaves
First printing ..... 205 unnumbered copies

UNCLASSIFIED

SECURITY CLASSIFICATION OF THIS PAGE (When Data Entered)

REPORT DOCUMENTATION PAGE	READ INSTRUCTIONS BEFORE COMPLETING FORM
1. REPORT NUMBER: NWC TP-5881	2. GOVT ACCESSION NO.
3. RECIPIENT'S CATALOG NUMBER	
4. TITLE (and Subtitle): EVALUATION OF THE HARPOON MISSILE SHOCK ENVIRONMENT DURING EJECTION LAUNCH BY AIRCRAFT LAUNCHERS.	5. TYPE OF REPORT & PERIOD COVERED: Final July 1973 — November 1975
	6. PERFORMING ORG. REPORT NUMBER: 2950, Project No. 157158
7. AUTHOR(s): Allan G. Piersol, Bolt Beranek and Newman Inc.	8. CONTRACT OR GRANT NUMBER(s): N6053D-75-M-5630
9. PERFORMING ORGANIZATION NAME AND ADDRESS: Bolt Beranek and Newman Inc., 21120 Vanowen Street, Canoga Park, CA 91303	10. PROGRAM ELEMENT, PROJECT, TASK AREA & WORK UNIT NUMBERS: AIRTASK A05P-204/2162/6000/00000
11. CONTROLLING OFFICE NAME AND ADDRESS: Naval Weapons Center, China Lake, CA 93555	12. REPORT DATE: February 1977
	13. NUMBER OF PAGES: 38
14. MONITORING AGENCY NAME & ADDRESS (if different from Controlling Office)	15. SECURITY CLASS. (of this report): Unclassified
	15a. DECLASSIFICATION/DOWNGRADING SCHEDULE

16. DISTRIBUTION STATEMENT (of this Report)

Approved for public release; distribution unlimited

17. DISTRIBUTION STATEMENT (of the abstract entered in Block 20, if different from Report)

18. SUPPLEMENTARY NOTES

19. KEY WORDS (Continue on reverse side if necessary and identify by block number)

Harpoon Ejection Shock Environment
High Frequency (Pyrotechnic Shock)
Missile Launch Ejection System
Maximax Shock Spectrum
Residual Shock Spectrum
High- and Low-Force Ejection Cartridges

20. ABSTRACT (Continue on reverse side if necessary and identify by block number)

See back of form.

DD FORM 1 JAN 73 1473 EDITION OF 1 NOV 65 IS OBSOLETE S/N 0102-014-6601

UNCLASSIFIED

SECURITY CLASSIFICATION OF THIS PAGE (When Data Entered)

389655

1B

(U) *Evaluation of the Harpoon Missile Shock Environment During Ejection Launch by Aircraft Launchers*, by Allan G. Piersol, Bolt Baranek and Newman Inc. China Lake, Calif., Naval Weapons Center, February 1977. 38 pp. (NWC TP 5881, publication UNCLASSIFIED.)

(U) A series of ground launch ejections of a Harpoon missile were performed to establish and evaluate the Harpoon ejection shock environment. The acceleration response of the missile was measured at 30 locations during various ejections from an MAU-9A/A and an Aero-7A-1 rack. The data were reduced to acceleration shock spectra covering a frequency range from 100 to 10 000 Hz. The results of the study produced considerable information concerning launch ejection shock environments of general interest. For example, the shock spectra of the response at all locations typically displayed a sharp increase in level in the frequency range around 800 Hz, which is well above the estimated frequency of the first flexural hoop mode of the missile shell. This frequency appears to be a significant dividing line for various other response characteristics. Increasing the clearance between the ejector foot and missile increased the response shock spectrum levels at frequencies above 800 Hz, but did not significantly increase the levels at lower frequencies. On the other hand, the response levels along the three orthogonal axes were not significantly different, on the average, at frequencies below 800 Hz, but were significantly different at the higher frequencies, with the highest response occurring in the vertical direction and the lowest in the axial direction. There was no significant difference in the missile response during ejections from the MAU-9A/A and Aero-7A-1 rack. However, increasing the force of the ejection cartridges did significantly increase the shock response of the missile at frequencies below 800 Hz. The shock response of the missile decreased greatly with distance from the point of impact. For example, the peak acceleration levels at locations only 10 inches from the point of impact were less than 20%, on the average, of the levels measured at the point of impact.

CONTENTS

INTRODUCTION

The dynamic response experienced by externally carried aircraft stores during launch ejection can pose a major reliability hazard to store equipment and structure. For example, the Walleye glide bomb has a history of guidance problems when high-force cartridges are used for launch ejection. As a result, restrictions have been placed on the cartridges used to eject the Walleye missiles. Similar restrictions have been placed on other ejection-launched stores. It follows that the shock environment induced by launch ejection is of considerable interest in current development programs of aircraft-launched weapons, including the Harpoon missile.

Various test programs have been performed in the past to measure the shock environment for aircraft-launched stores during ejection. In most cases, however, data were collected only at frequencies below 2.5 kHz. There have been two recent test programs involving the Antipersonnel-Antimaterial (APAM) and Mk 83 bombs where data were collected at frequencies up to 10 kHz. In both cases the dynamic response of the test items in the frequency range from 2.5 to 10 kHz was substantially greater than expected. These facts motivated an extensive launch ejection test program on the Harpoon missile that would provide shock response data at frequencies up to 10 kHz. This report summarizes the results of that test program and is believed to be of general interest.

TEST CONFIGURATIONS AND PROCEDURES

The Harpoon missile (AGM-84A) is an antiship missile designed to be launched from aircraft, surface ships, and submarines. The air-launched missile configuration is shown in Figure 1. The missile has a low-level cruse trajectory, active radar guidance, and terminal maneuvering to ensure maximum weapon effectiveness. During cruise it is powered by a turbojet sustainer engine.

TEST MISSILE CONFIGURATION

The missile configuration used for the tests simulated a prototype vehicle in size, weight, and CG. The total weight of the test vehicle was 1137 pounds (516 kg), with a CG located at missile station 83.6. No attempt was made to simulate wire bundles, valves, tubing, and other plumbing components; nor was secondary structure included, except where it was required to mount equipment packages. These items contribute very little mass and stiffness, and hence their absence should not significantly influence the shock response. All major equipment items were included in the test configuration. Some of the major components were structurally and mechanically the same as the real equipment, but not necessarily a functional device. Other major items were simulated, with the same mass, CG, and mounting configuration as the component being represented. A description of each missile section and equipment item included in the test vehicle follows.

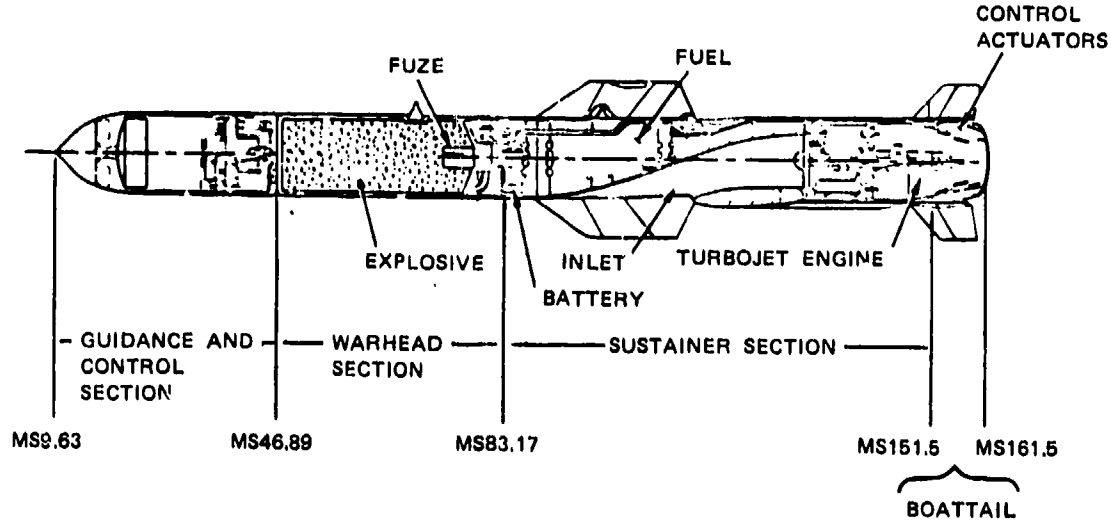

WINGSPAN, IN (m)	36.0 (0.914)
DIAMETER, IN (m)	13.5 (0.343)
SHIPBOARD LENGTH, IN (m)	180.0 (4.572)
SHIPBOARD WEIGHT, LB (kg)	1470.0 (666)
AIR–LAUNCH LENGTH, IN (m)	151.0 (3.835)
AIR–LAUNCH WEIGHT, LB (kg)	1150.0 (522)

FIGURE 1. Harpoon Missile.

Guidance Section. This section consisted of an actual radome structure, battery, and midcourse guidance unit (MGU), and a simulated altimeter. The seeker was a structural and mechanical representation of the actual seeker.

Test and Evaluation Section. The T&E section consisted of actual structure with all appropriate openings, doors, trays, and bulkheads, and simulated components. The T&E section simulated the weight and CG of the warhead section in the Harpoon missile, but not the stiffness. Specifically, the stiffness of the T&E section was in excess of that for the Harpoon integrated ordnance section. The two proximity fuzes were mass-simulated installations.

Sustainer Section. This section was composed of actual structure. The fuel tank was filled with water to simulate fuel weight. A spent real prototype engine was used; it was mounted to a prototype mounting ring and associated structure. A number of components that are normally mounted on the engine were not present. Lead ballast was attached to the engine to obtain the total appropriate weight and CG location.

Boattail Section. This section was actual structure with one real and three simulated actuators, and one real and three simulated control fins. The outboard location of each control fin CG from the missile mold line was not represented in the simulated fins.

DATA TRANSDUCERS

All acceleration measurements were made using Endevco Type 2292 and 2225 shock accelerometers in conjunction with Endevco Type 2713, 2718, and 2740 charge amplifiers. The accelerometers were mechanically mounted both externally and internally on the test missile, as shown in Figures 2 and 3 and as summarized in Table 1. In addition to the accelerometers, a pressure transducer was used to measure ejector rack cylinder pressure. Breakwires were used to record the time of rack hook release. The times at which the ejector foot impacted and separated from the missile were monitored by an electrical contact strip.

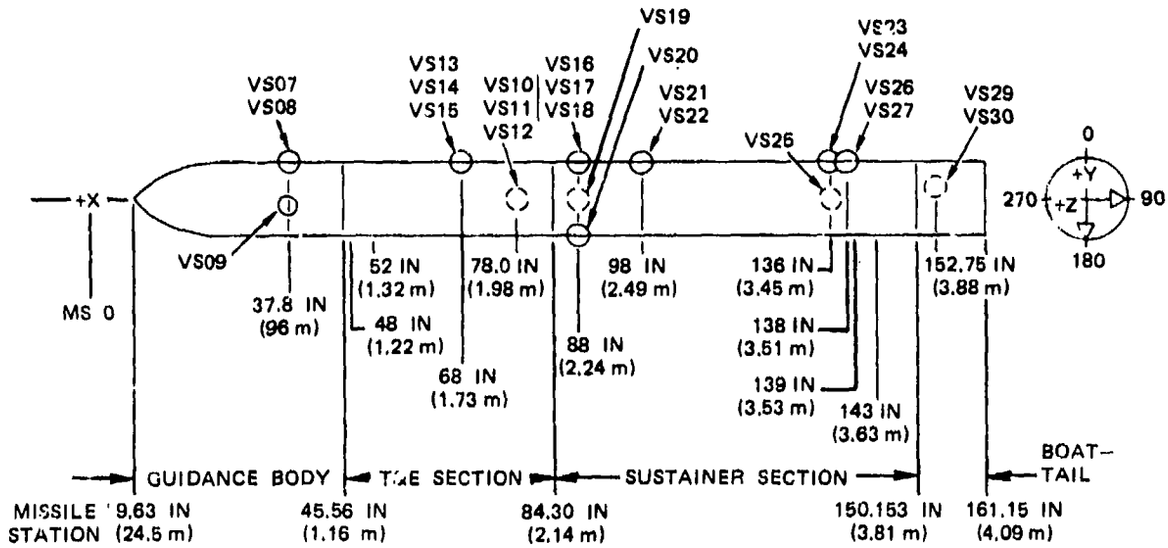

FIGURE 2. Location of External Accelerometers for Harpoon Ejection Tests.

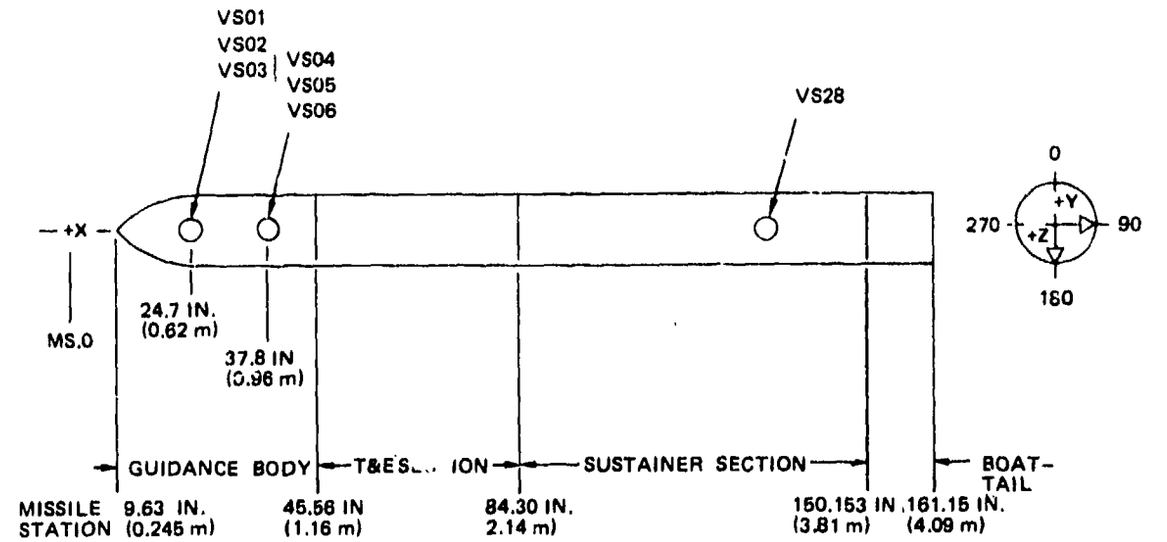

FIGURE 3. Location of Internal Accelerometers for Harpoon Ejection Tests.

TABLE 1. Summary of Transducer Locations for Harpoon Ejection Tests.
PS01 used pressure sensor; all others used accelerometers

No	Location	Direction	Station no. and orientation, deg	Internal or External	Range (zero to peak *gs*)
VS01	Seeker bulkhead	Axial	24.7	Internal	900
VS02	Seeker bulkhead	Lateral	24.7	Internal	900
VS03	Seeker bulkhead	Vertical	24.7	Internal	900
VS04	MGU flight control ring	Axial	37.8	Internal	1000
VS05	MGU flight control ring	Lateral	37.8	Internal	1000
VS06	MGU flight control ring	Vertical	37.8	Internal	1000
VS07	Guidance sect. structure	Axial	37.8,0	External	1000
VS08	Guidance sect. structure	Vertical	37.8,0	External	1000
VS09	Guidance sect. structure	Lateral	37.8,0	External	1000
VS10	Proximity fuze	Axial	78,90	External	5000
VS11	Proximity fuze	Lateral	78,90	External	5000
VS12	Proximity fuze	Vertical	78,90	External	5000
VS13	Forward attach lug	Axial	68,0	External	3000
VS14	Forward attach lug	Lateral	68,0	External	3000
VS15	Forward attach lug	Vertical	68,0	External	3000
VS16	Ejector foot impact	Axial	88,0	External	5000
VS17	Ejector foot impact	Lateral	88,0	External	5000
VS18	Ejector foot impact	Vertical	88,0	External	5000
VS19	T&E sect. structure	Lateral	88,90	External	5000
VS20	T&E sect. structure	Vertical	88,180	External	5000
VS21	Aft attach lug	Axial	98,0	External	5000
VS22	Aft attach lug	Vertical	98,0	External	5000
VS23	Engine sect. structure	Axial	136,0	External	1000
VS24	Engine sect. sturcture	Vertical	136,0	External	1000
VS25	Engine sect. structure	Lateral	136,90	External	1000
VS26	Engine sect. structure	Axial	138,0	External	1000
VS27	Engine sect. structure	Vertical	138,0	External	1000
VS28	Fuel controller	Vertical	Sustainer engine	Internal	1000
VS29	Control fin actuator	Axial	152.8,45	External	800
VS30	Control fin actuator	Radial	152.8,45	External	800
PS01	Rack cylinder pressure	. . .	On ejection rack	. . .	. .

EJECTION RACKS

Two different ejection racks were used for the tests, an Aero-7A-1 rack and a MAU-9A/A rack. Both rack assemblies consist of the following: a dual cartridge breech assembly, a hook assembly a star assembly group, and a sway brace assembly. Both racks accept the same cartridge combinations: one Mk 2 Mod 0 and one Mk 1 Mod 2 cartridge (this combination is hereafter referred to as the high-force cartridges) or two Mk 2 Mod 0 cartridges (hereafter referred to as the low-force cartridges). Nominal force-time histories for the two cartridge combinations are shown in Figure 4.

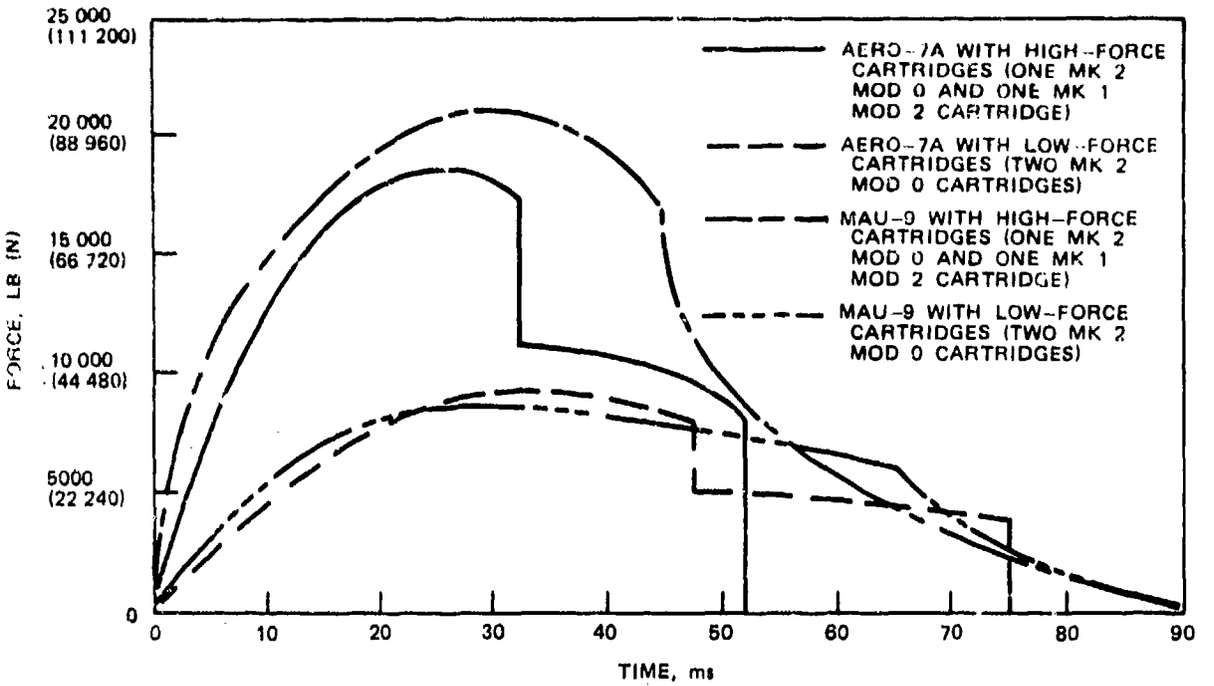

FIGURE 4. Nominal Ejection Force-Time Histories for Aero-7A-1 and MAU-9A/A Ejection Racks.

TEST FACILITY

The ejection tests were conducted at the Ground Ejection Test Facility, Pacific Missile Test Center, Point Mugu, Calif. The missile was allowed to free-fall approximately 6 feet (2 meters) after ejection before being arrested by restraining rope. All of the signal conditioning equipment was adjacent to the stand and hard-wired to the missile. The data were recorded in a data acquisition van located adjacent to the test stand. Figure 5 illustrates the test setup.

TEST PROCEDURE

The missile was installed on the ejection rack to simulate an actual aircraft installation. The cartridges were installed, the rack was armed, and a firing countdown was initiated. The tape recorders were turned on about 5 seconds before the ejection. After each ejection the missile was inspected for damage and was then reinstalled on the ejection rack. The restraining ropes were replaced, the instrumentation was again checked out, precalibrated, etc., and the above sequence was repeated. The first three tests were performed primarily for equipment checkout and calibration. The test sequence was as shown in Table 2.

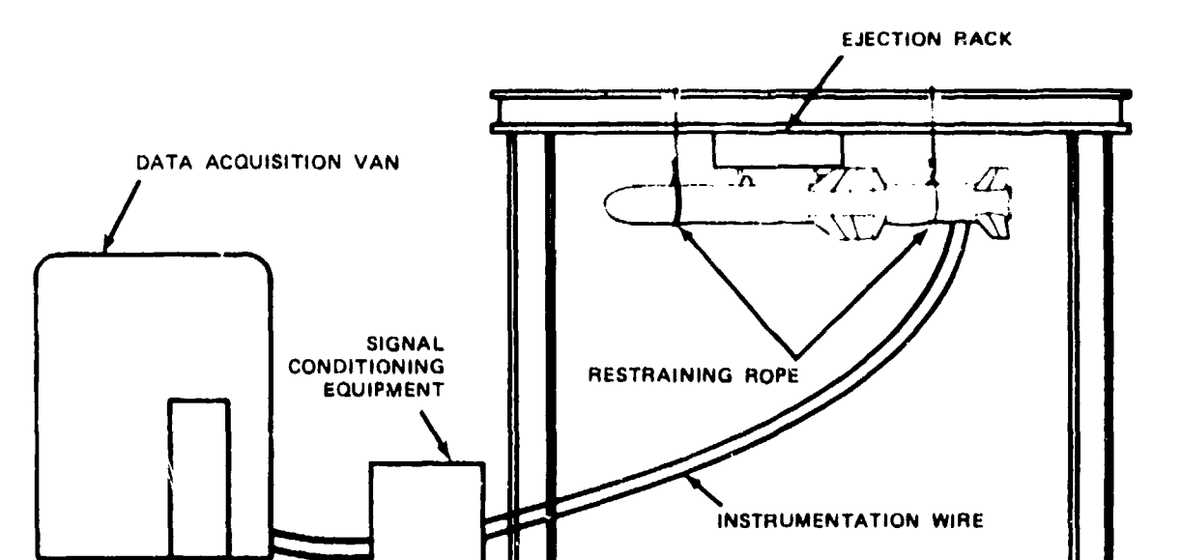

FIGURE 5. Harpoon Ejection Test Stand and Setup.

TABLE 2. Test Sequence for Harpoon Ejection Tests.

Test no.	Rack used	Ejector foot clearance	Ejector foot instrumentation	Cartridges used
1[a]	MAU-9A/A	Normal[b]	Yes	Low-force
2[a]	MAU-9A/A	Normal	No	Low-force
3[a]	MAU-9A/A	Normal	No	Low-force
4	MAU-9A/A	Normal	Yes	Low-force
5	MAU-9A/A	Normal	Yes	Low-force
6	MAU-9A/A	1/4 in. (6.4 mm)	Yes	Low-force
7	Aero-7A-1	Normal	Yes	Low-force
8	Aero-7A-1	Normal	Yes	Low-force
9	Aero-7A-1	Normal[c]	No	Low-force
10	Aero-7A-1	Normal	No	High-force
11	Aero-7A-1	Normal	No	High-force

[a]Equipment checkout and calibration tests.
[b]Normal clearance generally less than 1/16 in. (1.6 mm) (first detent).
[c]A repeat of Tests 7 and 8 with the ejector foot instrumentation (electrical contact strip) removed.

ANALYSIS PROCEDURES

The acceleration transients measured at various locations on the Harpoon missile during the simulated ejections were evaluated in terms of significant transient events and peak acceleration levels. The acceleration-time records were reduced to response (shock) spectra for more detailed evaluation using an SD 320 analyzer. Selected records were also reduced to energy spectra. (For the benefit of those readers who may not be familiar with these analysis procedures, a brief review and discussion are presented in Appendix A.)

EXPERIMENTAL RESULTS

The basic results of the Harpoon missile ejection test consist of acceleration-time histories, peak acceleration values, energy spectra, and shock spectra at the various measurement locations. Peripheral results include measurements of the ejection rack cylinder pressure, the time of contact and separation between the rack ejector foot and the missile, and the time of the rack hook release. Pertinent characteristics of these results are summarized in the following sections.

ACCELERATION-TIME HISTORIES AND RELATED PARAMETERS

Figure 6 shows a typical time history of an acceleration response that was measured on the Harpoon structure near the point of the ejector foot impact during a low-force ejection from the MAU-9A/A rack. Note that the history displays three distinct transient events, the first initiating at

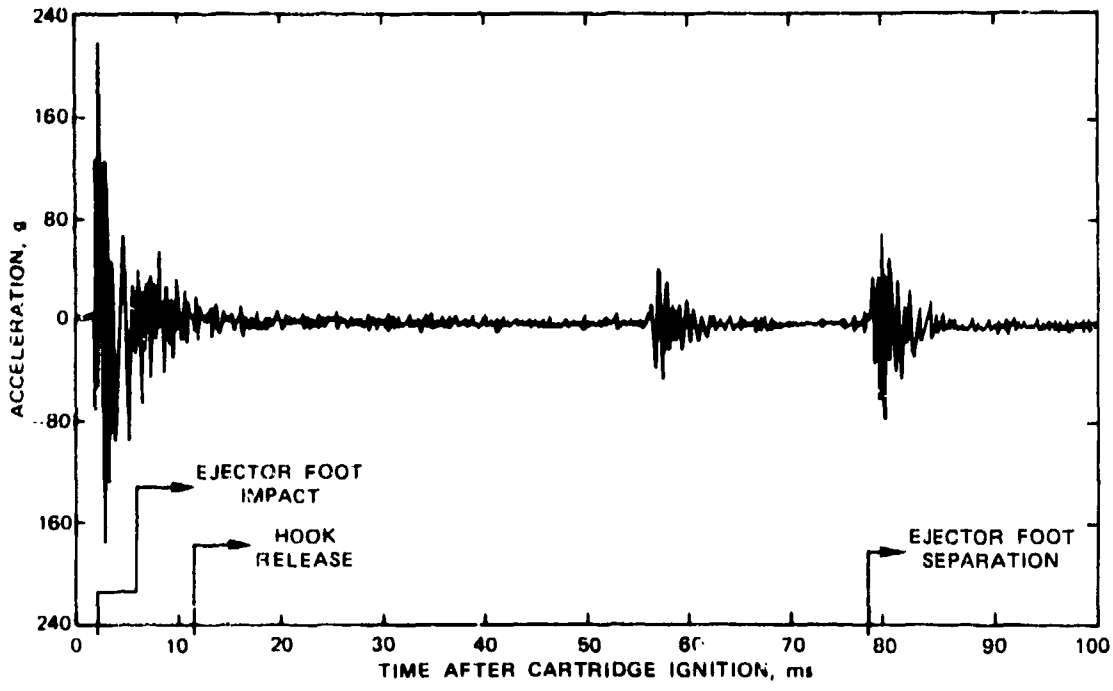

FIGURE 6. Acceleration-Time History at Ejector Foot Location (VS18) During Ejection Test 4 (MAU-9A/A Rack With Low-Force Cartridges).

about 2 ms, the second at about 56 ms, and the third at about 78 ms after cartridge ignition. The first event is due to the initial impact of the ejector foot on the missile. The third event reflects the final separation of the missile from contact with the ejector foot.

The source of the second event at about 56 ms is uncertain, but it appears that it may be related to a discontinuity in the ejection rack thrust, or perhaps even a momentary separation between the ejector foot and the missile. The event is present in the histories at all locations during all ejections. It occurs at about 47 ms after cartridge ignition during ejections from the Aero-7A-1 rack with the low-force cartridges, and at about 39 ms with the high-force cartridges. The vertical acceleration-time history for the latter case at the point of ejector foot impact is shown in Figure 7. Although of uncertain origin, this event between the initial impact and final separation is assumed to be physically significant and hence is included in the calculation of shock and energy spectra.

At locations more widely separated from the point of ejector foot impact, the acceleration-time histories are more complex. Figure 8 shows the vertical acceleration response measured on the guidance section structure during the same ejection that produced the data in Figure 6. Note that the same three events seen in Figure 6 are present at this location as well, but the responses have lower peak levels and are more spread in time. In particular, the initial transient starting at about 2 ms appears to maintain its strength up to about 15 ms, and then build up again between 20 and 25 ms. This is believed to represent the influence of flexural waves propagating from the point of impact down the missile shell at their group velocity (estimated to be about 600 ft/s (183 m/s) at the predominant frequency of about 700 Hz). For example, in the forward section of the missile at about 700 Hz, one would expect a flexural wave to pass the guidance measurement location at about 7 ms after impact, and reflect back off the nose past this same position at about 15 ms after impact. This is reasonably consistent with the results shown in Figure 8.

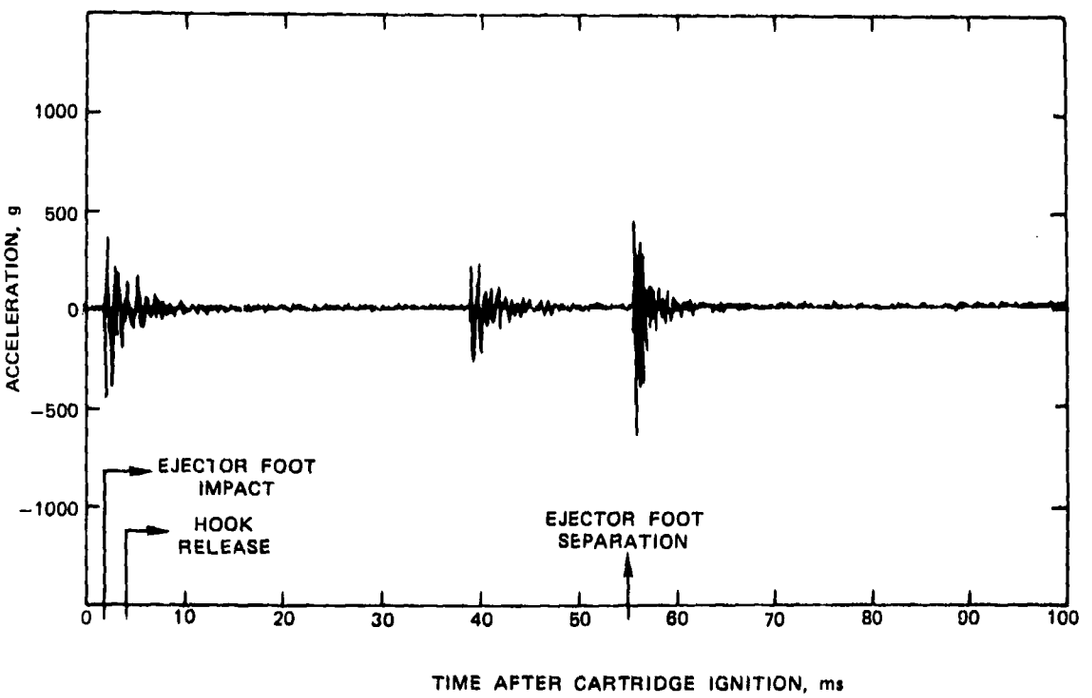

FIGURE 7. Acceleration-Time History at Ejector Foot Location (VS18) During Ejection Test 11 (Aero-7A-1 Rack With High-Force Cartridges).

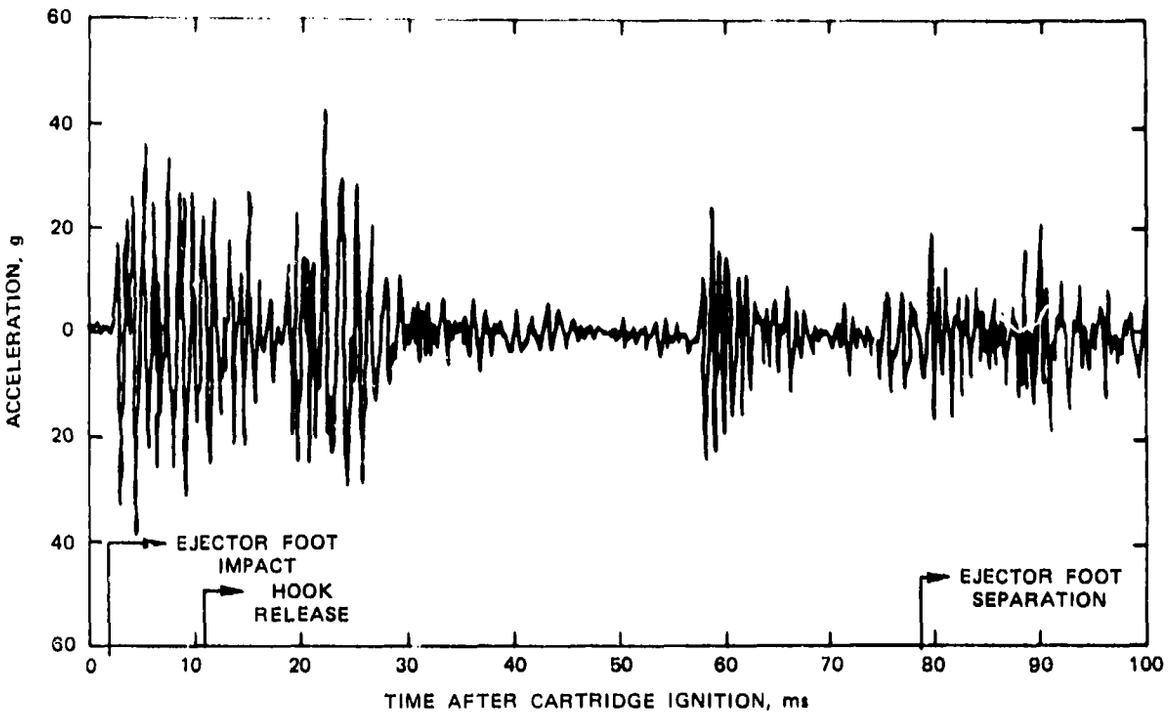

FIGURE 8. Acceleration-Time History at Guidance Section Location (VS08) During Ejection Test 4 (MAU-9A/A Rack With Low-Force Cartridges).

PEAK ACCELERATION RESULTS

The peak values of the acceleration-time histories recorded at the various measurement locations during Tests 4 through 11 are presented in Table 3. Note that the peak acceleration levels vary dramatically with type of rack, cartridge combination, and structural location. In general, the peak accelerations diminish rapidly with distance from the point of ejector foot impact, as will be discussed further in the "Evaluation of Results" section.

ENERGY SPECTRA RESULTS

A typical energy spectrum of the acceleration response is presented in Figure 9. This particular energy spectrum was computed from the acceleration-time history shown previously in Figure 7, using only that segment covering the separation transient from 55 to 62 ms. Since the separation transient in these tests approximates a unit step input, the energy spectrum at any location is closely related to the square of the frequency response function of the missile structure between that location and the impact location, as suggested by Equation (A-5) in the Appendix A. Hence the various significant peaks in the energy spectrum shown in Figure 9 represent important normal modes of the missile structure. For example, there is a peak at about 1000 Hz, which probably represents a strongly excited hoop mode of the missile shell. The peak at about 3000 Hz undoubtedly represents another strongly excited hoop resonance.

TABLE 3. Peak Acceleration Levels Measured During Harpoon Ejection Tests.
Tests 4 through 9: low-force cartridges. Tests 10 and 11: high-force cartridges.

No.	Location	Direction	Peak acceleration in *gs* for tests 4 through 11							
			4 MAU-9A/A	5 MAU-9A/A	6 MAU-9A/A	7 Aero-7A-1	8 Aero-7A-1	9 Aero-7A-1	10 Aero-7A-1	11 Aero-7A-1
VS01	Seeker bulkhead	Axial	12	12	12	23	12	13	15	19
VS02	Seeker bulkhead	Lateral	12	12	15	13	10	15	13	14
VS03	Seeker bulkhead	Vertical	10	10	20	18	18	...	30	20
VS04	MGU flight control ring	Axial	...	...	83	...	...	...	...	...
VS05	MGU flight control ring	Lateral	40	50	57	125	85	108	58	27
VS06	MGU flight control ring	Vertical	30	23	19	50	45	60	55	45
VS07	Guidance sect. structure	Axial	24	22	52	45	35	55	45	45
VS08	Guidance sect. structure	Vertical	43	40	64	55	75	65	110	98
VS09	Guidance sect. structure	Lateral	88	65	75	123	87	87	90	100
VS10	Proximity fuze	Axial	52	34	63	...	45	60	75	50
VS11	Proximity fuze	Lateral	...	30	50	...	40	57	63	40
VS12	Proximity fuze	Vertical	90	84	144	...	80	...	160	100
VS13	Forward attach lug	Axial	32	42	38	...	55	55	60	...
VS14	Forward attach lug	Lateral	19	16	36	...	35	35	50	33
VS15	Forward attach lug	Vertical	42	34	78	...	60	60	94	55
VS16	Ejector foot impact	Axial	100	116	248	...	190	250	260	240
VS17	Ejector foot impact	Lateral	140	152	250	...	160	280	450	300
VS18	Ejector foot impact	Vertical	218	176	368	...	500	500	625	650
VS19	T&E sect. structure	Lateral	248	200	576	475	400	600	420	970
VS20	T&E sect. structure	Vertical	205	224	315	350	550	400	660	...
VS21	Aft attach lug	Axial	92	86	118	115	67	137	110	93
VS22	Aft attach lug	Vertical	92	100	150	160	95	142	130	...
VS23	Engine sect. structure	Axial	30	22	42	30	13	33	30	80
VS24	Engine sect. structure	Vertical	52	40	80	97	60	85	65	70
VS25	Engine sect. structure	Lateral	72	46	100	60	...	65	55	50
VS26	Engine sect. structure	Axial	38	35	54	45	20	40	50	...
VS27	Engine sect. structure	Vertical	48	52	80	70	35	90	70	60
VS28	Fuel controller	Vertical	7	9	16	11	6	13	20	...
VS29	Control fin actuator	Axial	33	24	54	30	20	...	40	33
VS30	Control fin actuator	Radial	60	44	108	46	33	57	...	50

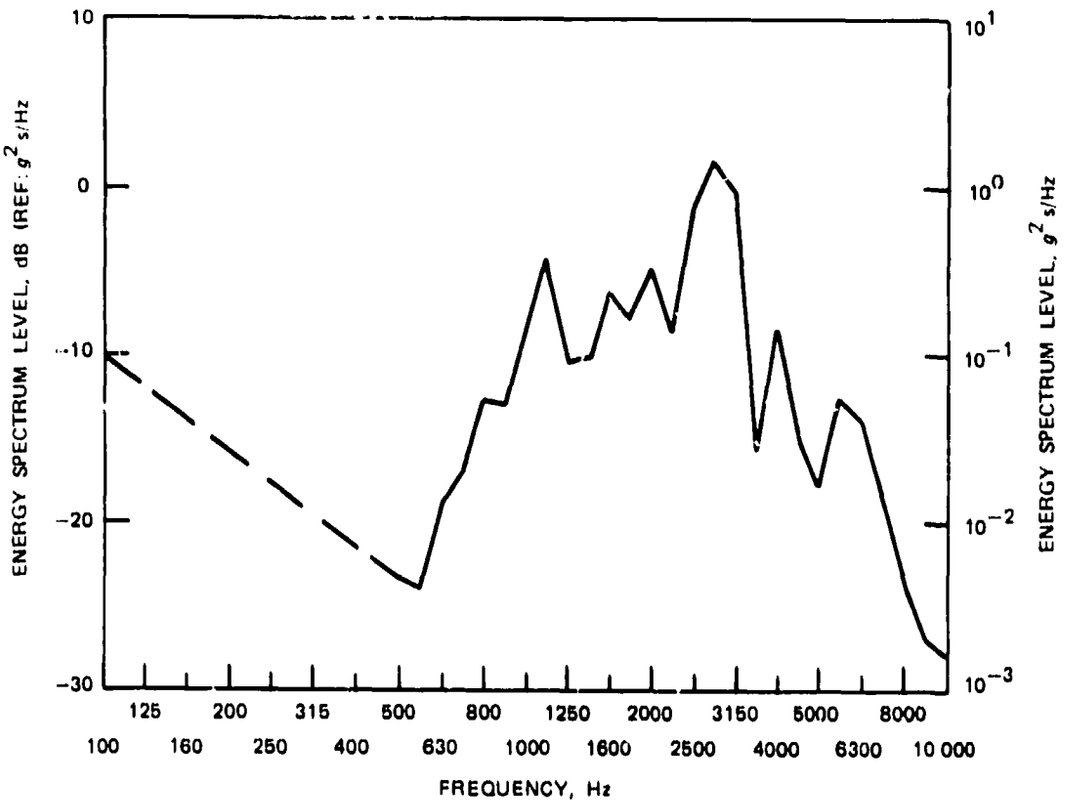

FIGURE 9. Energy Spectrum at Ejector Foot Location (VS18) For Separation Transient During Ejection Test 11 (Aero-7A-1 Rack With High-Force Cartridges).

SHOCK SPECTRA RESULTS

A typical set of shock spectra for the acceleration response are presented in Figures 10 and 11. The two spectra in Figure 10 are maximax results for two different damping ratios, specifically, Q = 10 and Q = 100. The spectra in Figure 11 represents the positive and negative shock spectra for Q = 100. All of the spectra were computed from the acceleration-time history previously presented in Figure 7.

In Figure 10 it is seen that the shock spectra levels are somewhat higher for the more lightly damped case, as would be expected. In both cases, Q = 10 and Q = 100, the spectra display peaks at about the same frequencies. Furthermore, the frequencies of these significant peaks correspond in many cases to the frequencies of peaks previously observed in the energy spectrum shown in Figure 9. In broad terms, however, the shock spectrum values tend to rise and the energy spectrum values tend to fall with increasing frequency. This observation is consistent with the basic difference in the characteristics of shock and energy spectra, as is discussed in Appendix A.

In Figure 11 it is seen that the positive and negative shock spectra of the transient are similar at frequencies above 600 Hz. At the lower frequencies, however, the positive spectrum levels sometimes exceed the negative levels by a significant amount. This reflects the fact that the basic transient associated with the rack ejector foot striking the missile is in the positive (downward) direction.

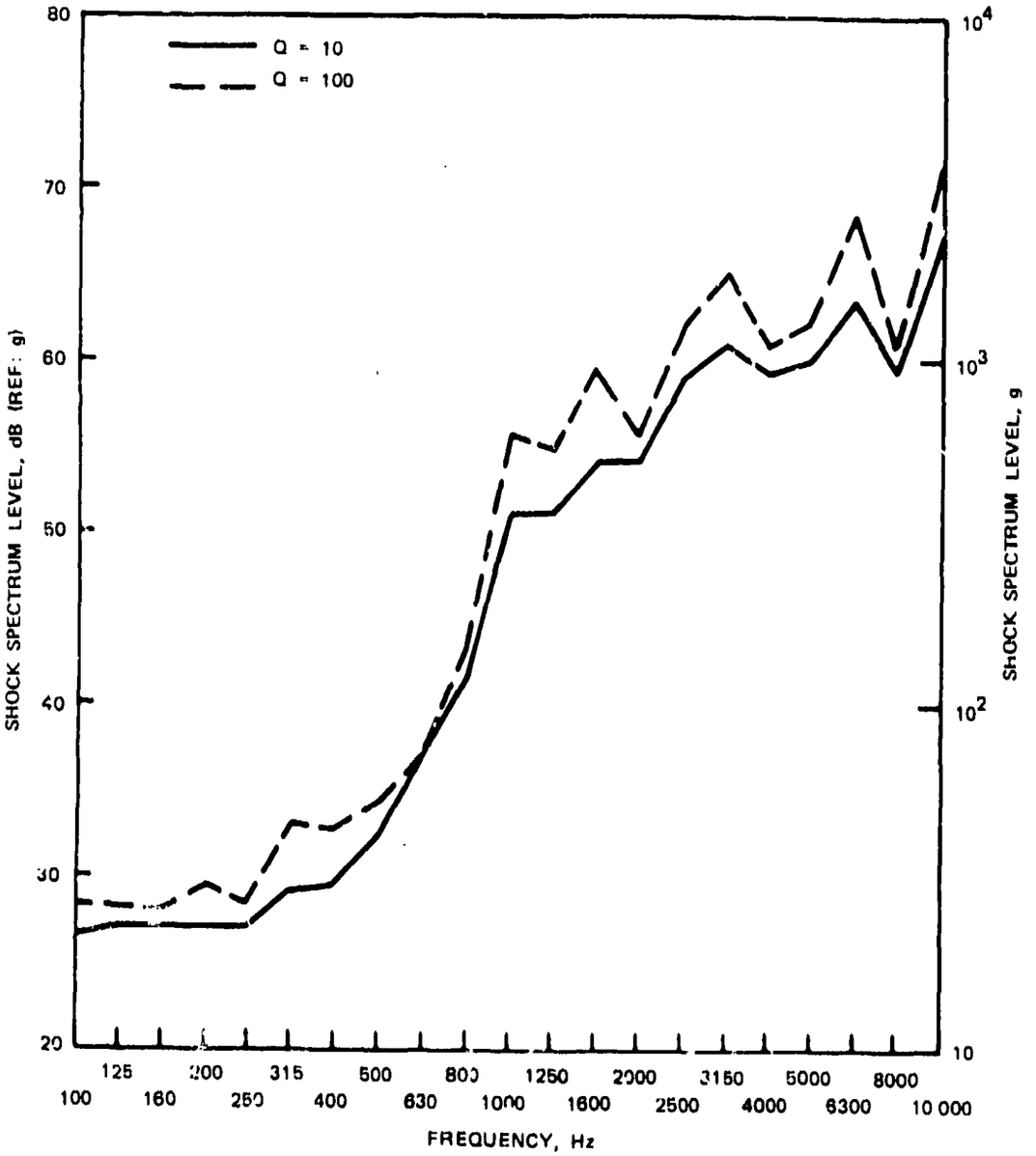

FIGURE 10. Maximax Shock Spectra for Q = 10 and Q = 100 at Ejector Foot Location (VS18) During Ejector Test 11 (Aero-7A-1 Rack With High-Force Cartridges).

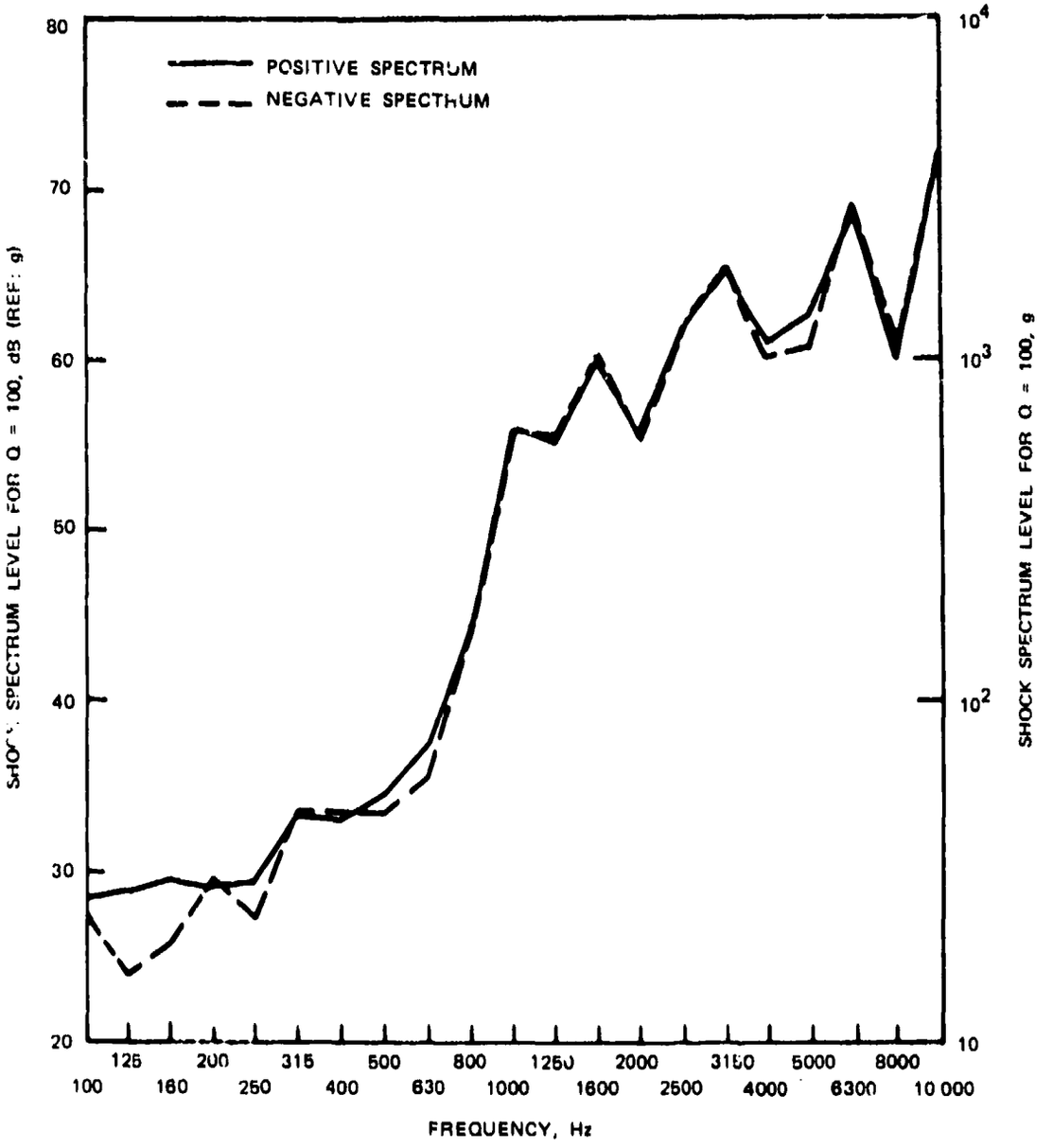

FIGURE 11. Positive and Negative Shock Spectra for Q = 100 at Ejector Foot Location (VS18) During Ejection Test 11 (Aero-7A-1 Rack With High-Force Cartridges).

EVALUATION OF RESULTS

Various aspects of the shock spectra test results are of interest, including variations with repeated ejections, ejector foot instrumentation, foot clearance, rack type, cartridge size, measurement direction, and measurement location. Such variations were investigated using the shock spectra results and the peak acceleration data summarized in Table 3. To permit the evaluations to be performed in an efficient manner, the shock spectra of interest were first converted to average levels in contiguous 1/3-octave bandwidths. Both the shock spectra values and the peak acceleration values were also converted to dB referenced to 1 g (dB = 20 log g). This was done so a given percentage difference in acceleration values would be weighted equally in the statistical studies, independent of the absolute acceleration values. All statistical evaluations were performed using the well-known UCLA biomedical statistical data analysis computer programs.

Many of the evaluations involved comparisons of different cases based upon average shock spectra values. These average spectra were computed separately for each 1/3-octave band by averaging over all locations where data were available for the cases being compared in that plot. Due to the wide dynamic range of the shock spectra data, accurate shock spectra values were not always retrieved at all locations, particularly in the frequency range below 1000 Hz. Since this problem was most common at those locations displaying relatively low response levels, the average values computed in the frequency range below 1000 Hz often tended to be biased upwards. However, in any given figure to follow, the same locations were used for all cases of interest to compute the average values in a given 1/3-octave band, and hence the results within that figure are directly comparable.

VARIATIONS AMONG REPEATED EJECTION TESTS

Referring back to Table 2, the test missile was ejected at least twice from each of the three ejection rack-cartridge configurations. The rack performance from one test to another for a given configuration was quite consistent, at least as measured by the chamber pressure-time histories. This fact is demonstrated in Figure 12, which shows the pressure-time histories for Tests 4, 5, and 6, all

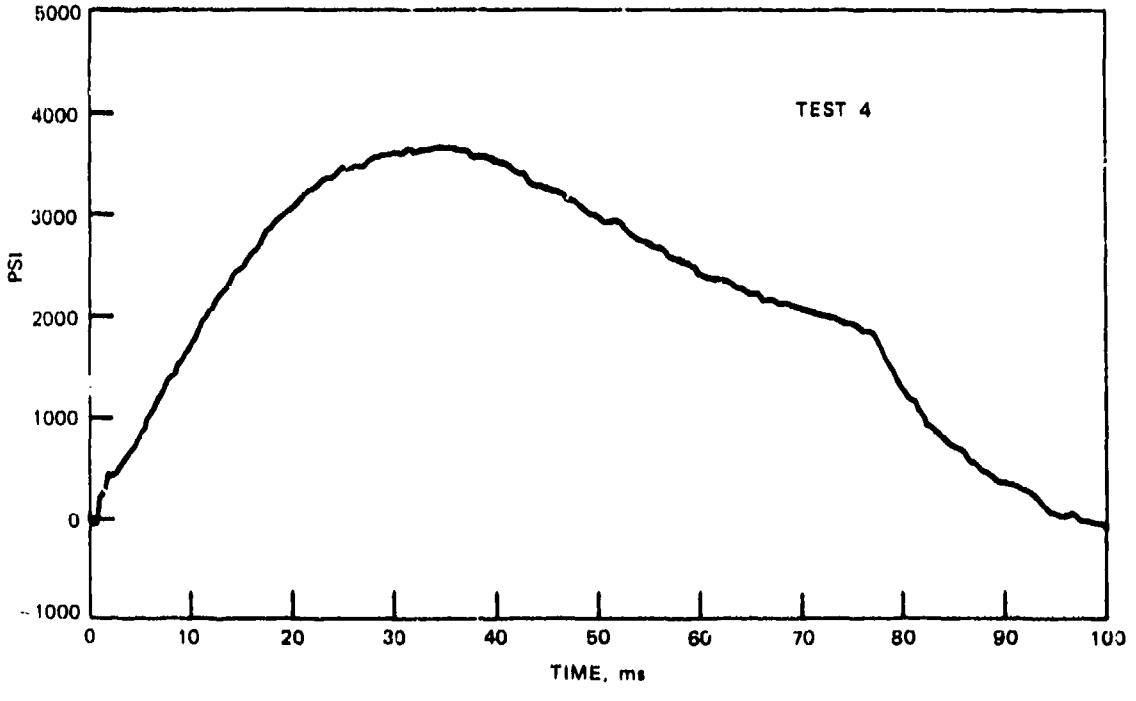

FIGURE 12. Rack Chamber Pressure-Time Histories for Repeated Ejections During Tests 4, 5, and 6 (MAU-9A/A Rack With Low-Force Cartridges).

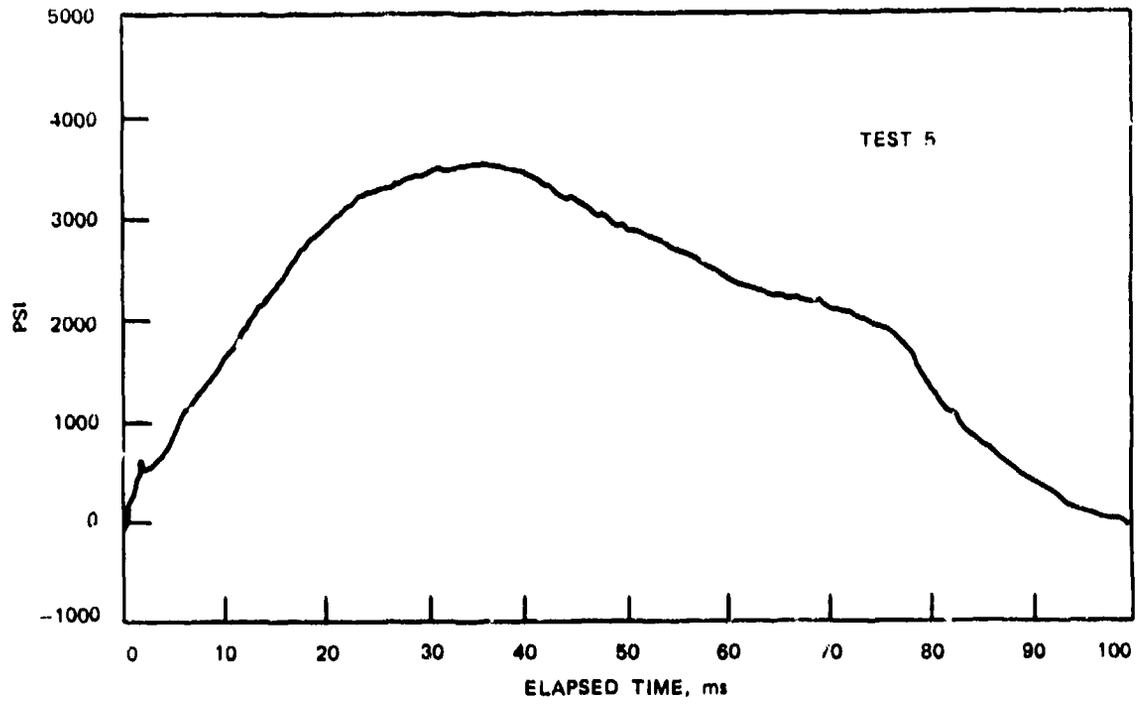

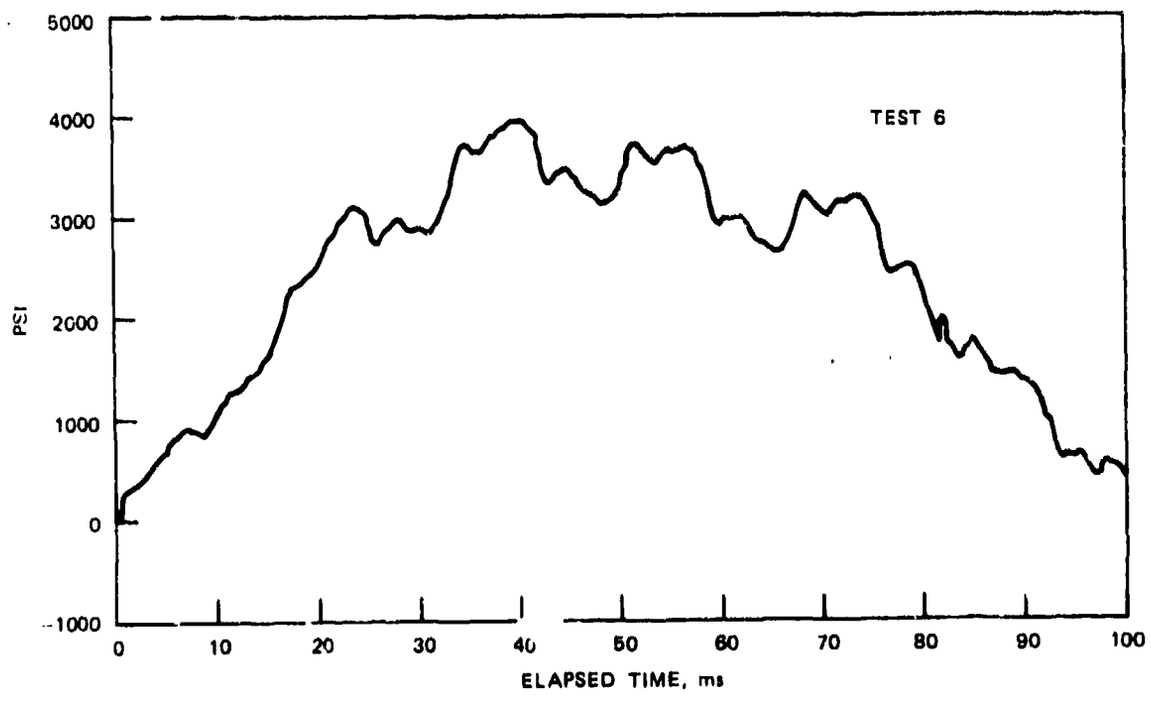

FIGURE 12. (Contd.)

involving the MAU-9A/A rack with the low-force cartridges. Note that the ejector foot clearance was increased for Test 6, which probably explains the less stable result for this test.

The peak acceleration values measured at the various locations during repeated ejections under identical conditions are also in close agreement, on the average, as demonstrated in Table 4. In both comparisons, the difference in the average peak acceleration levels is not sufficient to be considered statistically significant at the $\alpha = 1\%$ level of significance, based upon a conventional Student "t" test of differences.

The shock spectra values measured at specific locations on the missile sometimes differ between repeated tests by up to 2:1 (6 dB) at certain frequencies. On the average, however, the shock spectra for repeated tests are in good agreement (within anticipated statistical variations), at least in the frequency range below 4000 Hz, as shown in Figure 13. At frequencies above 4000 Hz, discrepancies are observed between the average shock spectra values up to 3.5 dB. These discrepancies are slightly outside the range of expected statistical variations and may represent the sensitivity of the high frequency response of the missile to the exact manner in which the ejector foot initially strikes the missile structure. In any case the repeatability of the test results is considered acceptable.

TABLE 4. Comparison of Average Peak Acceleration Levels for Repeated Ejection Tests.

Test no.	Test configuration	Average of peak accelerations dB	Average difference dB	Standard deviation, dB	Sample size	Significant difference at 1% level, dB
4	1[a]	33.46				
			0.81	1.75	28	0.91
5	1	32.65				
6	1	37.10	...[c]	...[c]	...[c]	...[c]
10	2[b]	37.80				
			0.94	3.51	23	2.05
11	2	36.86				

[a]MAU-9A/A rack with low-force cartridges, normal ejector foot clearance, and ejector foot instrumentation

[b]Aero-7A-1 rack with high-force cartridges, normal ejector foot clearance, and no ejector foot instrumentation

[c]Not analyzed.

VARIATIONS WITH EJECTOR FOOT INSTRUMENTATION

Some of the ejection tests were performed with an electrical contact strip mounted on the missile to identify the times of foot-missile contact and separation. For Tests 9, 10, and 11 this instrumentation was removed. During the initial checkout tests (1, 2, and 3), it was determined by visual inspection of acceleration-time histories that the ejector foot instrumentation had no significant influence on the resulting missile structural response. However, the peak acceleration data for Tests 7 and 8 versus 9, which were identical ejections except for the ejector foot instrumentation, suggest that the electrical contact strip might have caused a slight reduction in the resulting shock loads, at least as measured by peak acceleration levels on the missile structure. The average of the peak acceleration levels measured at all locations during Tests 7 and 8 were about 1.5 dB lower, on the average, than the peak accelerations recorded during Test 9. This constitutes a statistically significant difference at the 1% level of significance but not a major difference in physical terms. Nevertheless, the possibility of some minor influence due to the ejector foot instrumentation should be kept in mind when comparing the results of tests performed with and without the instrumentation.

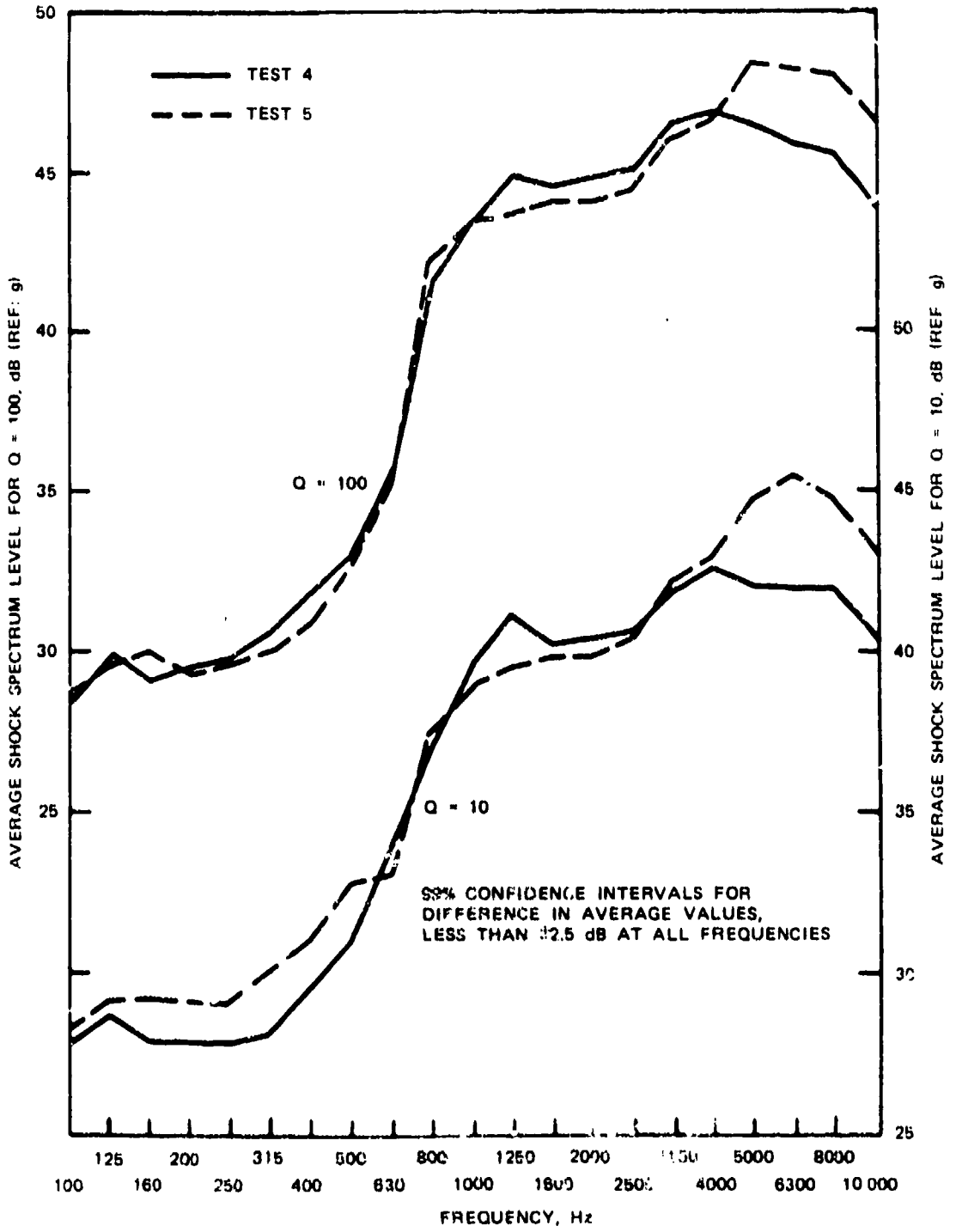

FIGURE 13. Shock Spectra Average Over All Locations for Repeated Ejections From MAU-9A/A Rack Using Low-Force Cartridges. Average levels at frequencies below 1000 Hz computed over those locations of most intense response only.

VARIATIONS WITH EJECTOR FOOT CLEARANCE

Of the three ejection tests performed with the MAU-9A/A rack using the low-force cartridges (Tests 4, 5, and 6), Test 6 was conducted with the ejector foot-missile clearance increased to 1/4 inch (6.4 mm) from the normal 1/16 inch (1.6 mm) or less. The peak acceleration data in Table 4 indicate a significant increase in levels due to the increased clearance. Specifically, the average of the peak accelerations with the increased clearance is 37.1 dB, as compared to 33.0 dB with normal clearance. However, most of this increased structural response with increased clearance occurs in the frequency range above 800 Hz as illustrated in Figure 14, which presents the average shock spectra of the response accelerations during Tests 4 and 5 versus Test 6 for Q = 10 and Q = 100. Note that the shock spectrum levels for the increased clearance case are no more than 1.8 dB higher than for the normal clearance case at frequencies below 800 Hz. Above 800 Hz, however, the levels for the increased clearance case are over 5 dB higher at some frequencies, well beyond the limits of anticipated statistical variations. Therefore, it must be concluded that the shock response of the missile structure at frequencies above 800 Hz is dependent upon the clearance between the ejector foot and the missile.

VARIATIONS WITH Q FACTOR

Shock spectra values for any given transient are a function of the damping ratio; a smaller damping ratio (larger Q) will produce larger shock spectra values. This dependence on Q for the Harpoon shock data is illustrated in Figure 15, which presents the average spectra for all locations during Tests 4 and 5 computed for Q = 10 and Q = 100. Note that there is no significant statistical error in the indicated differences between the Q = 10 and Q = 100 curves, since both curves were computed from identical histories. Figure 15 shows that the shock spectrum values for Q = 100 exceed the values for Q = 10 by less than 1.5 dB at frequencies below about 800 Hz. At higher frequencies, however, the difference increases to about 4.5 dB. This result indicates that the Harpoon structure tends to "ring" for a longer period of time at the higher frequencies; i.e., the structural response to the ejection shock tends to decay much more rapidly at the lower frequencies. This reaction is generally characteristic of the response of lightly damped structures to sharp impact loads.

VARIATIONS WITH MEASUREMENT DIRECTION

Figure 16 shows the differences in the average shock spectra levels for Q = 100 along the three orthogonal axes during Tests 4, 5, and 6. These results indicate that the shock spectrum levels at most frequencies are lowest in the axial direction and highest in the vertical direction, as would be expected for a cylindrical structure subjected to a shock load normal to its axis. However, the differences in the spectral values among the three orthogonal axes are not dramatic, particularly at the lower frequencies. For example, in the frequency range below 800 Hz, the differences among the three axes are always less than 3 dB, as compared to anticipated statistical variations of about ±2 dB for each measurement.

VARIATIONS WITH TYPE OF RACK

The average shock spectra values for Q = 10 for ejections from the MAU-9A/A rack with low-force cartridges and similar data from the Aero-7A-1 rack are compared in Figure 17. Note that the general shapes of the average shock spectra for the two cases are similar, but the spectral values

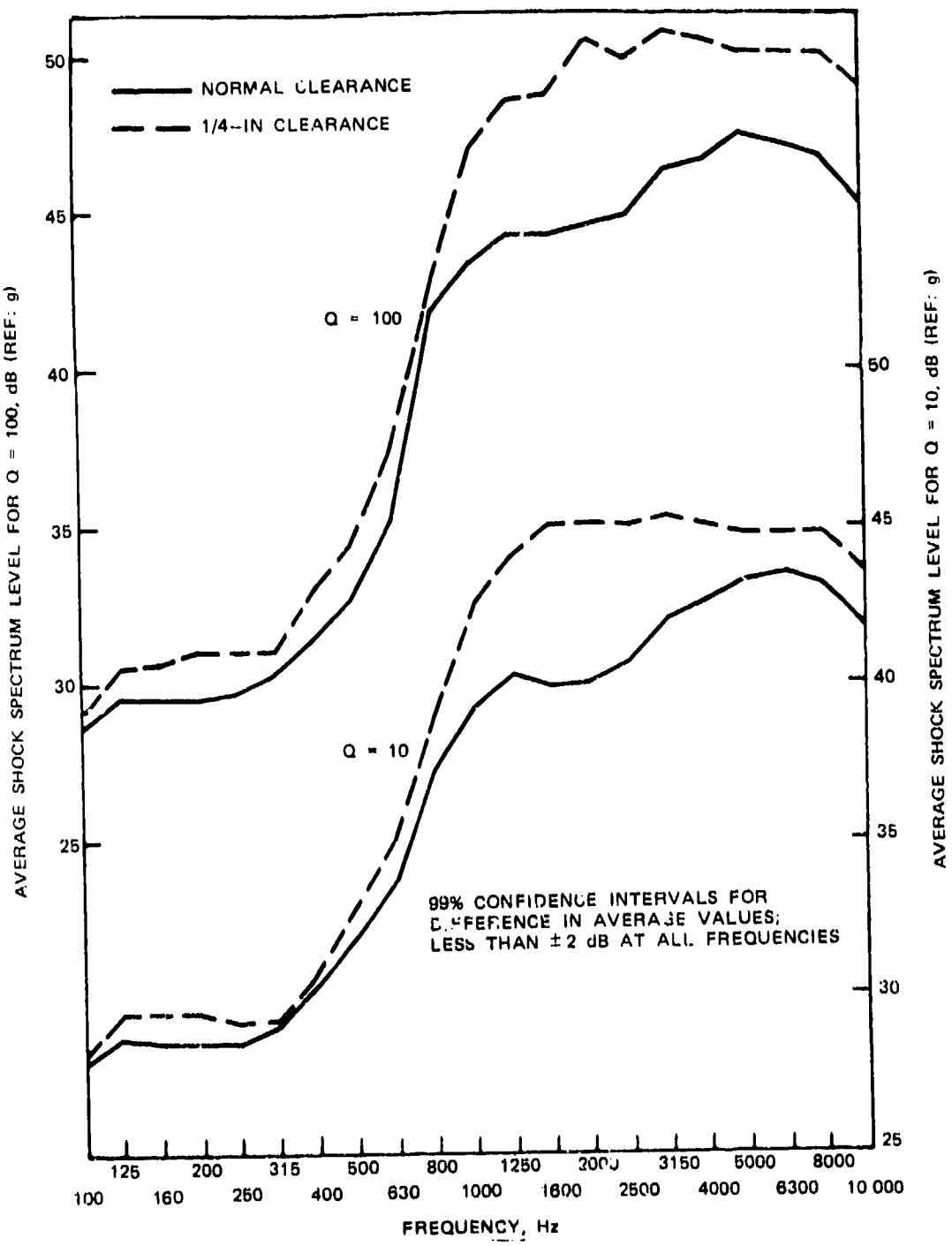

FIGURE 14. Shock Spectra Average Over All Locations for Ejections During Tests 4, 5, and 6 (MAU-9A/A Rack Using Low-Force Cartridges With Normal and Increased Ejector Foot Clearance). Average levels at frequencies below 1000 Hz computed over those locations of most intense response only.

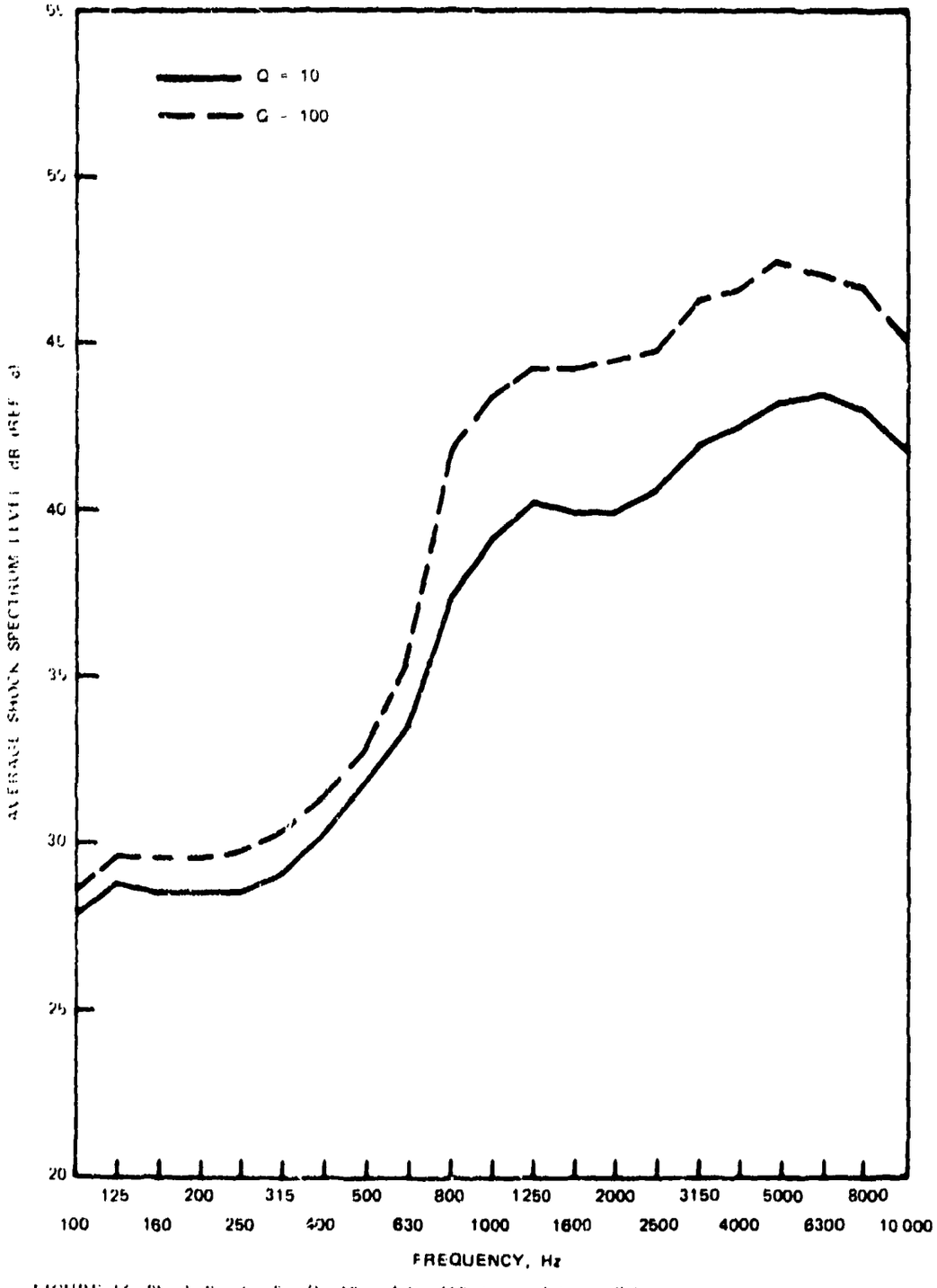

FIGURE 15. Shock Spectra for Q = 10 and Q = 100 Averaged Over All Locations for Ejections During Tests 4 and 5 (MAU-9A/A Rack Using Low-Force Cartridges). Average levels at frequencies below 1000 Hz computed over those locations of most intense response only.

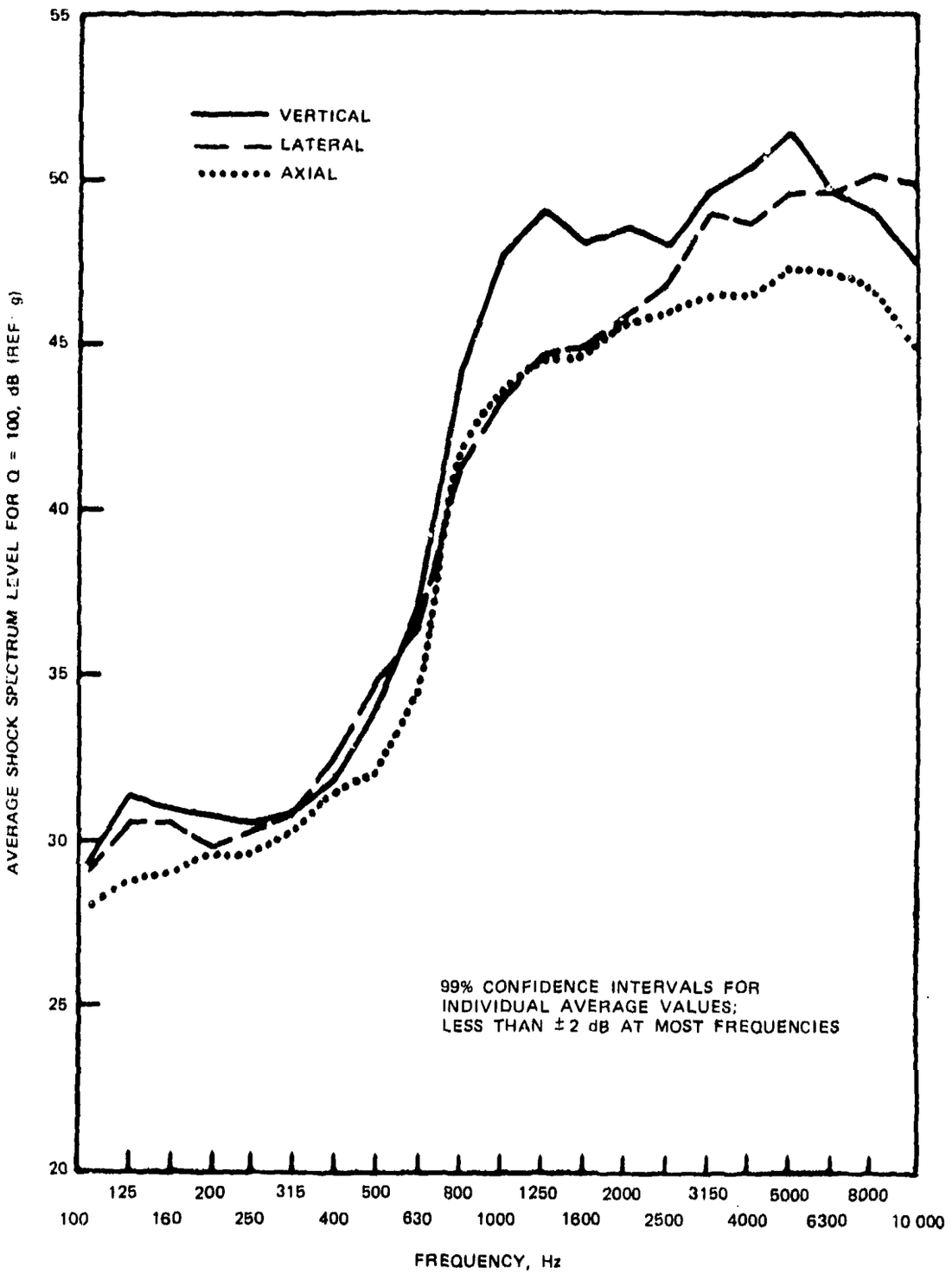

FIGURE 16. Shock Spectra for Q = 100 Averaged Over All Locations Along Each Orthogonal Axis for Ejections During Tests 4, 5, and 6 (MAU-9A/A Rack Using Low-Force Cartridges). Average levels at frequencies below 1000 Hz computed over those locations of most intense response only.

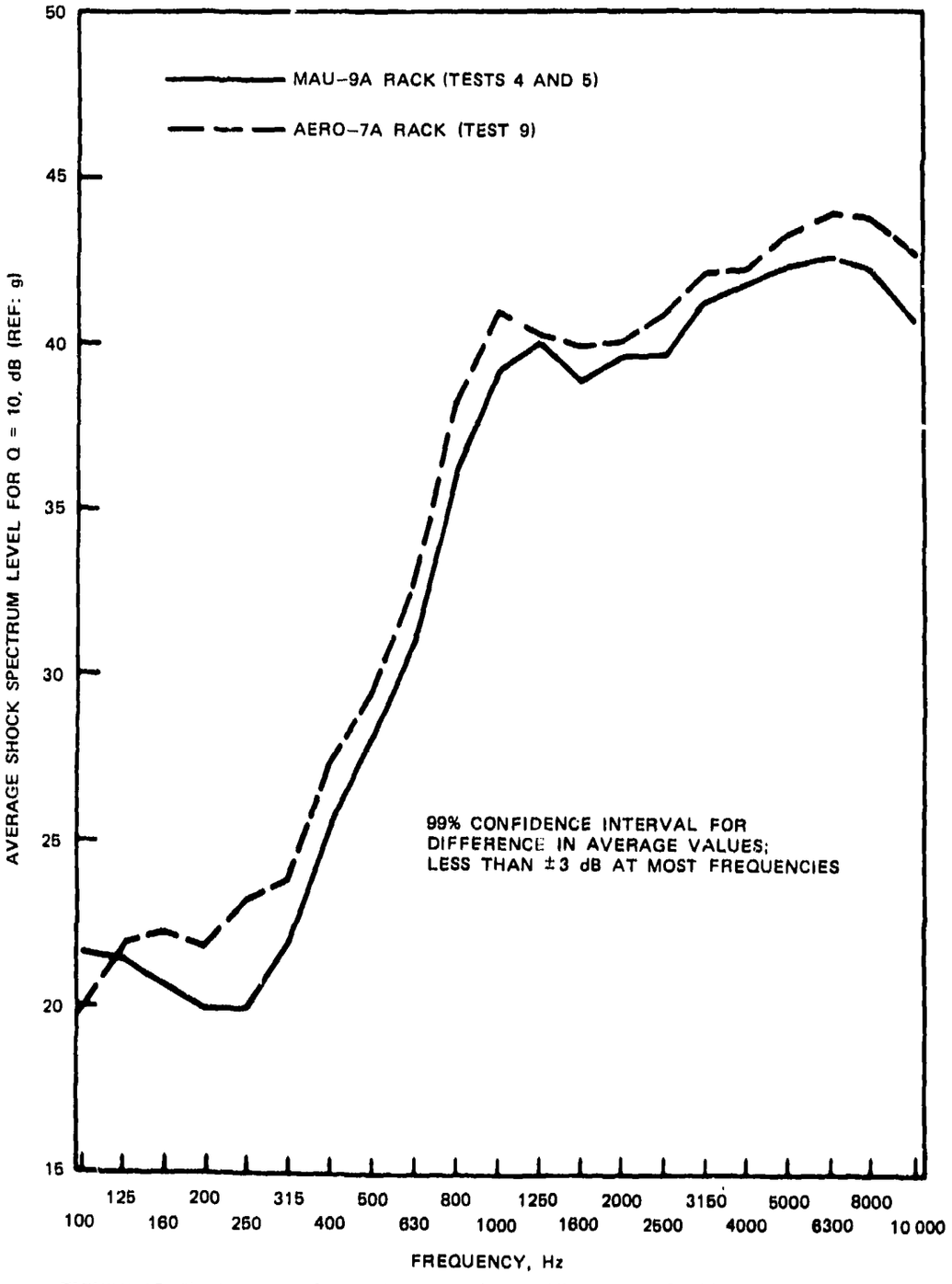

FIGURE 17. Shock Spectra for Q = 10 Averaged Over All Locations for Ejections During Tests 4 and 5 (MAU-9A/A and Aero-7A-1 Racks Using Low-Force Cartridges).

for the Aero-7A-1 rack ejection are consistently higher by 1 to 3 dB at all frequencies, except for the lowest band at 100 Hz. Although this discrepancy is usually within the range of anticipated statistical variations for any given frequency band, the consistency of the discrepancy over all frequencies suggests that the shock loads were actually higher by a small amount (1.3 dB on the average) for the Aero-7A-1 ejection. It should be noted, however, that the MAU-9A/A ejections (Tests 4 and 5) were performed with the ejector foot instrumentation installed, whereas the Aero-7A-1 ejection was performed without this instrumentation. A possible explanation for the indicated difference in levels is given in a later section called "Comparisons Based Upon Energy Spectra."

On the other hand, the peak acceleration data in Table 4 tend to support the conclusion that the shock response of the missile during ejection from the Aero-7A-1 rack, even with the ejector foot instrumentation, was somewhat more severe than during ejection from the MAU-9A/A rack, at least in the region of the ejector foot impact. Furthermore, the nominal force-time histories for ejections from the two racks, as shown in Figure 4, indicate that the peak ejection force is slightly higher for the Aero-7A-1 rack, which could translate into slightly higher shock response levels. On balance, however, any differences that may exist in the missile shock environment due to ejections from the MAU-9A/A versus the Aero-7A-1 rack do not appear to be sufficiently great to warrant separate consideration of the two racks.

VARIATIONS WITH SIZE OF CARTRIDGES

Figure 18 compares the average shock spectra values for $Q = 10$ for an ejection from the Aero-7A-1 rack with the low-force and the high-force cartridges. It should be mentioned that the dynamic range of the analysis for the measurements was quite good, and hence even the low frequency values represent an accurate average of almost all the 30 measurements made on the missile structure.

It is clear from Figure 18 that the missile shock response is more severe for the ejection with the high-force cartridges, particularly in the frequency range below 800 Hz. The average shock spectrum levels are consistently about 4 dB higher in this frequency range when the high-force cartridges are used. Noting that the nominal ejection force with the high-force cartridges is about twice as great as for the low-force cartridges, one might have expected the shock response levels to have doubled, i.e., to have increased by 6 dB. The lack of a full 6-dB increase in levels with the doubling of ejection force probably reflects the influence of nonlinearities in the response of the missile structure to intense shock loads.

VARIATIONS WITH STRUCTURAL LOCATIONS

The 30 measurements of the missile shock response during the various ejection tests were made at 10 specific structural locations over the length of the missile, as shown in Table 1 and Figures 2 and 3. It is now of interest to evaluate how the missile shock response varied from one location to another. This variation is illustrated in Figure 19 in terms of peak acceleration levels versus the missile station number for the locations. The peak acceleration levels averaged over the available measurements at each location are shown separately for the three basic ejection rack-cartridge configurations tested.

The results in Figure 19 clearly demonstrate that the missile shock response diminishes very rapidly with axial distance from the point of ejection, as would be expected. For example, from the point of ejector foot impact to the proximity fuze, a distance of only 10 inches (8.3 m), the peak

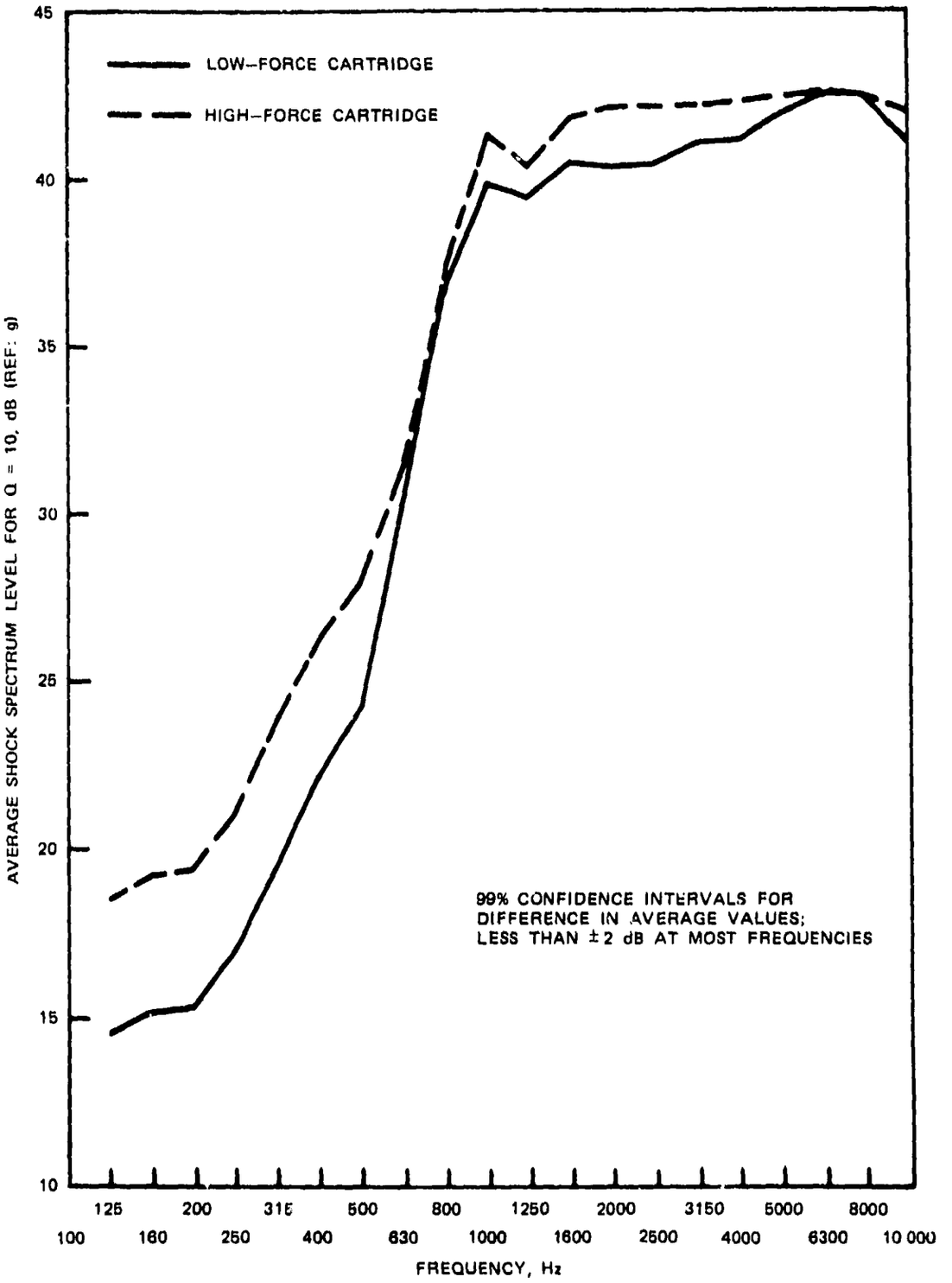

FIGURE 18. Shock Spectra for Q = 10 Averaged Over All Locations for Ejections (Aero-7A-1 Rack Using Low- and High-Force Cartridge Combinations).

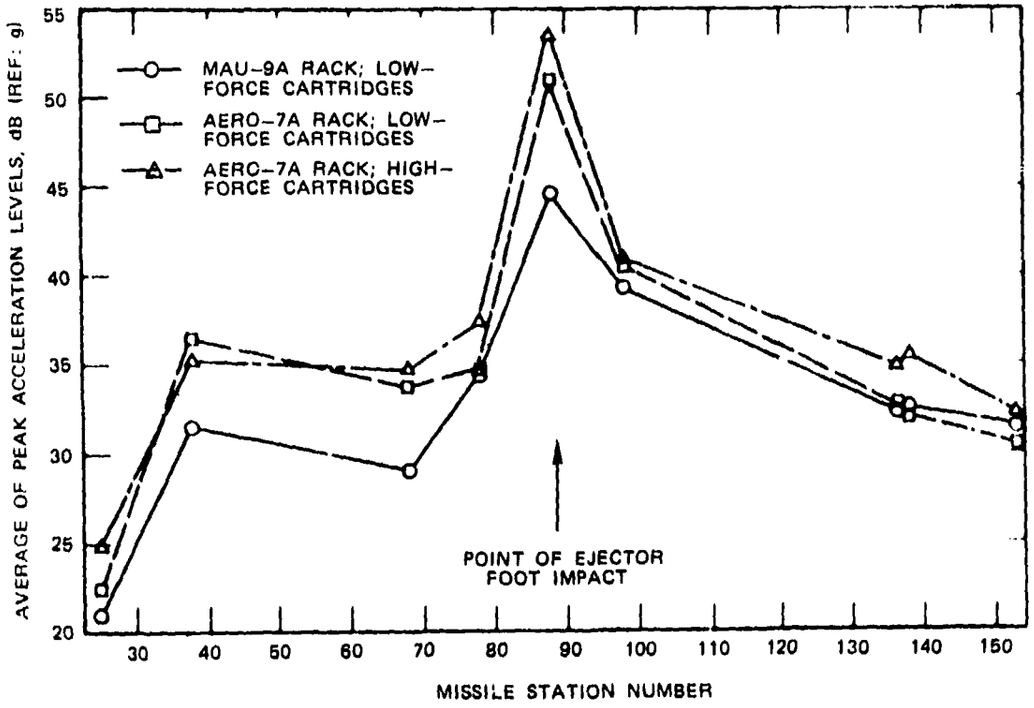

FIGURE 19. Peak Acceleration Response Levels Versus Missile Station Number for Various Ejection Rack and Cartridge Combinations.

acceleration levels during ejections from the Aero-7A-1 rack drop by 16 dB (a ratio of over 6:1). From the ejector foot to the seeker bulkhead, the drop is over 28 dB (a ratio of 25:1). In other words, the seeker section at station 25 sees acceleration peaks that are only 4% as great as those measured at station 88, the point of impact. About 10 dB of this reduction occurs over the last 10 inches (8.3 m) between the guidance section and the seeker section.

This dramatic variation in the shock response with structural location is illustrated by the shock spectra data shown in Figures 20 and 21. Here the shock spectra average of available measurements at each location are shown for ejection from the Aero-7A-1 rack with high-force cartridges. The shock spectra for locations at station 88 (the ejector foot and T&E section structure) far exceed those at all other locations and frequencies. The seeker section at the forward end of the missile displays a uniquely low shock response spectrum at frequencies above 200 Hz. The shock spectra at other locations scatter between these two extremes.

COMPARISONS TO EQUIPMENT DESIGN CRITERIA

The environmental design criteria for the Harpoon missile[1] specify that the missile equipment should withstand a half-sine-wave shock load with a duration of 0.5 ms and an amplitude of 385 to 1100 g, depending upon the location along the length of the missile. The peak acceleration levels

[1]Naval Air Systems Command. *Environmental Design Criteria for the AGM-84A/RGM-84A Missile (Harpoon.)* Washington, D.C., 1973. (XAS-2381A.)

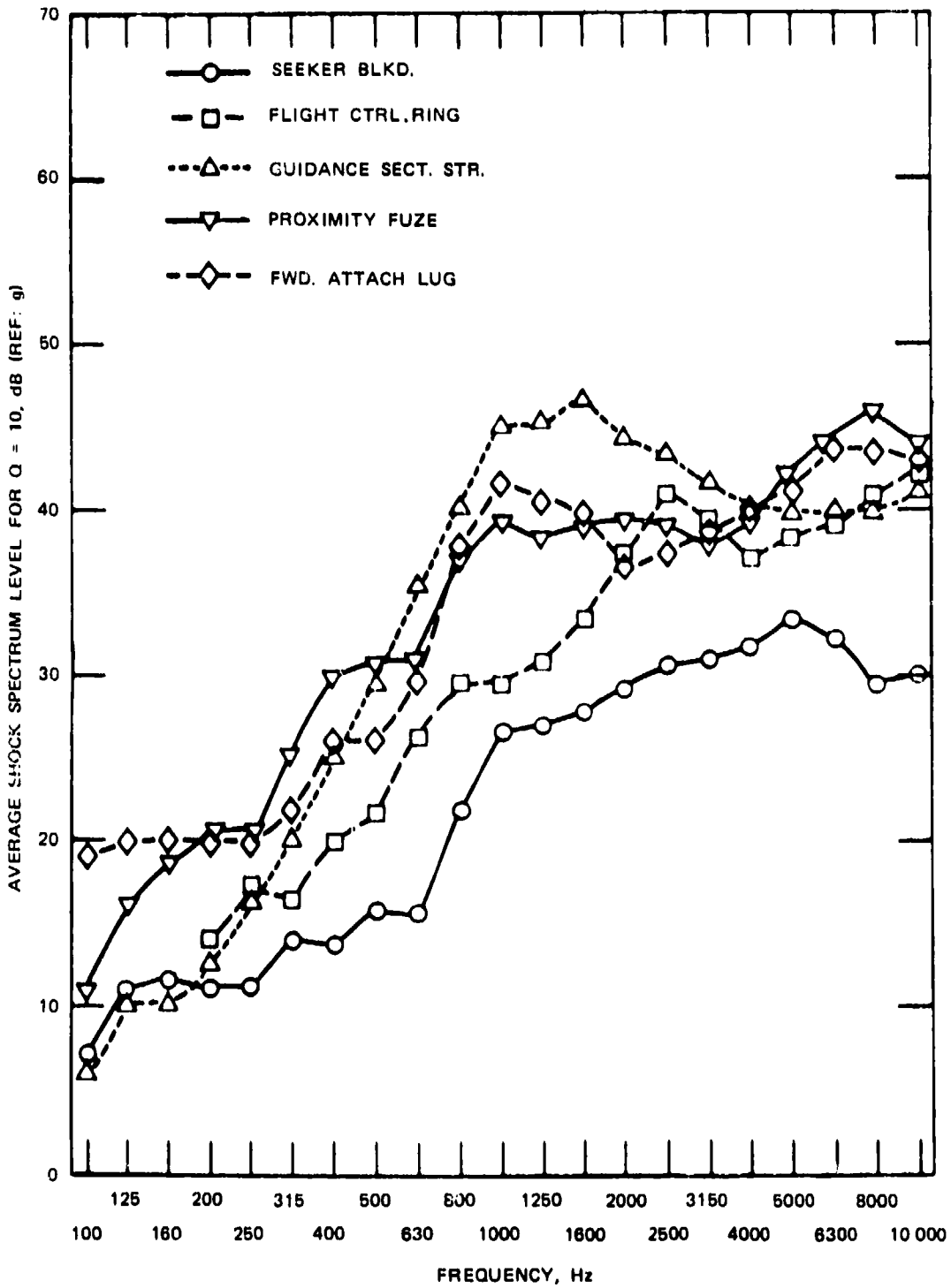

FIGURE 20. Shock Spectra for Q = 10 Averaged Over Three Axes at Various Locations for Ejection (Aero-7A-1 Rack Using High-Force Cartridges).

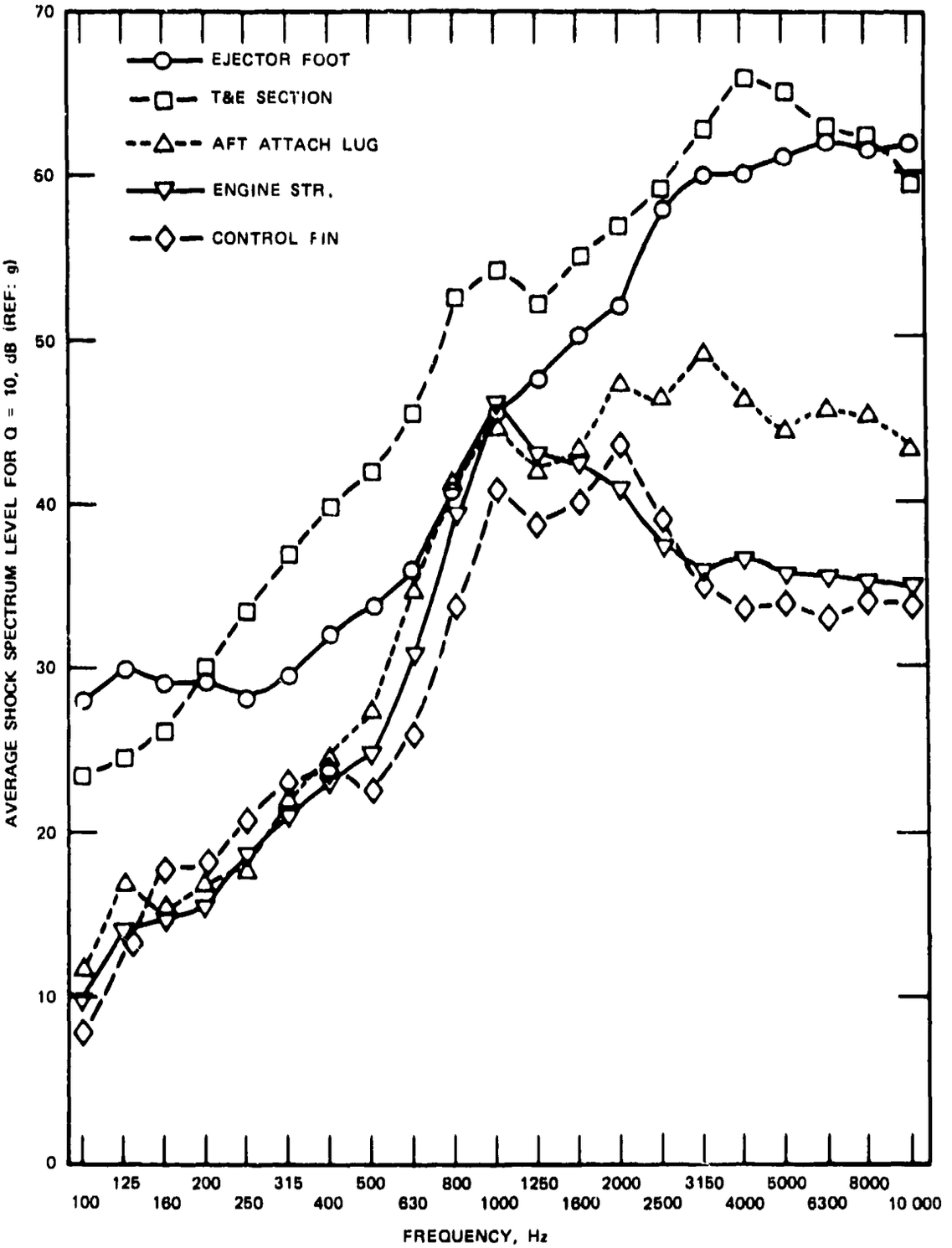

FIGURE 21. Shock Spectra for Q = 10 Averaged Over Three Axes at Various Locations for Ejection (Aero-7A-1 Rack Using High-Force Cartridges).

measured during the test ejections, as summarized in Table 3, are all well below the peak acceleration level of the equipment design criterion for each location. However, as is discussed in Appendix A, the peak accelerations in themselves do not provide a fully definitive comparison between dissimilar transient acceleration-time histories. A comparison based upon a frequency-dependent parameter is generally more meaningful. Such equipment comparisons are now made using both shock and energy spectra for the ejection from the Aero-7A-1 rack using the high-force cartridges. Based upon the evaluations of the equipment comparisons, this case generally represents the most severe launch ejection shock condition tested.

COMPARISONS BASED UPON SHOCK SPECTRA

In Figures 22, 23 and 24 shock spectra for the equipment design criteria are compared to the measured shock spectra of the missile response at three key equipment locations. In these figures the measured shock spectrum shown for each location represents the maximum spectral value computed in all directions at that location, independently for each 1/3-octave frequency band, during ejection from the Aero-7A-1 rack with the high-force cartridges.

From Figures 22, 23, and 24 it is seen that the ejection shock response of the Harpoon equipment, as measured in terms of a Q = 10 shock spectrum, falls well below the design requirements at all locations considered. It appears reasonable to conclude that the Harpoon equipment design criteria for ejection shock loads are conservative.

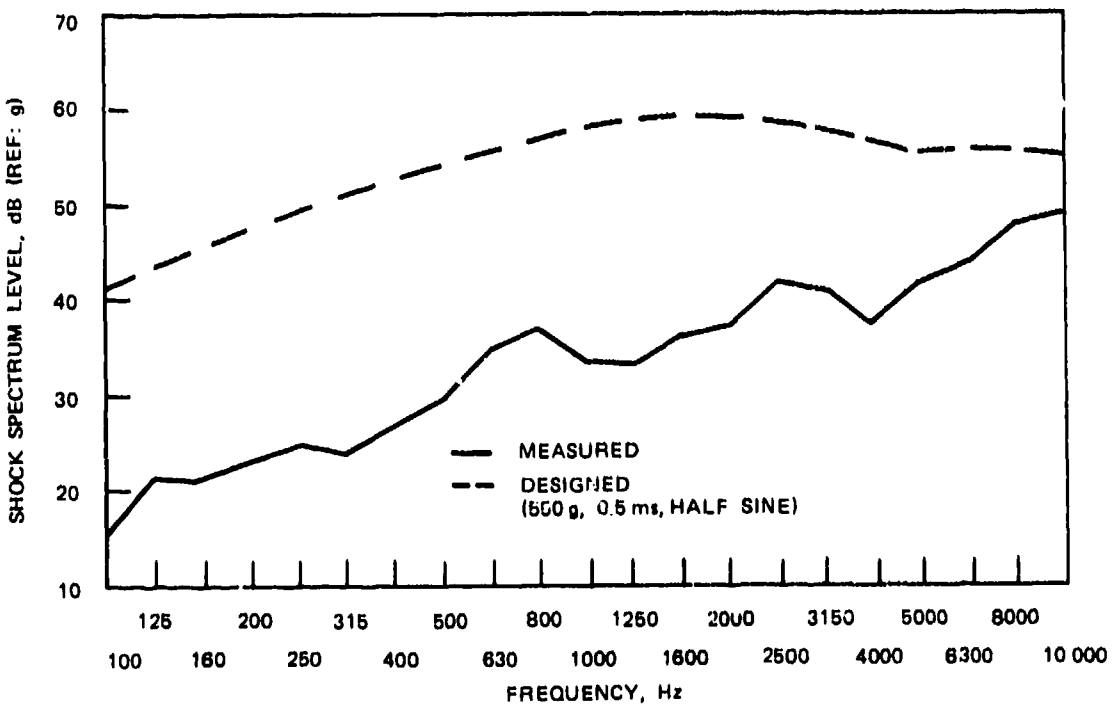

FIGURE 22. Comparison of Q = 10 Shock Spectrum Levels and Design Criterion for the Midcourse Guidance Unit.

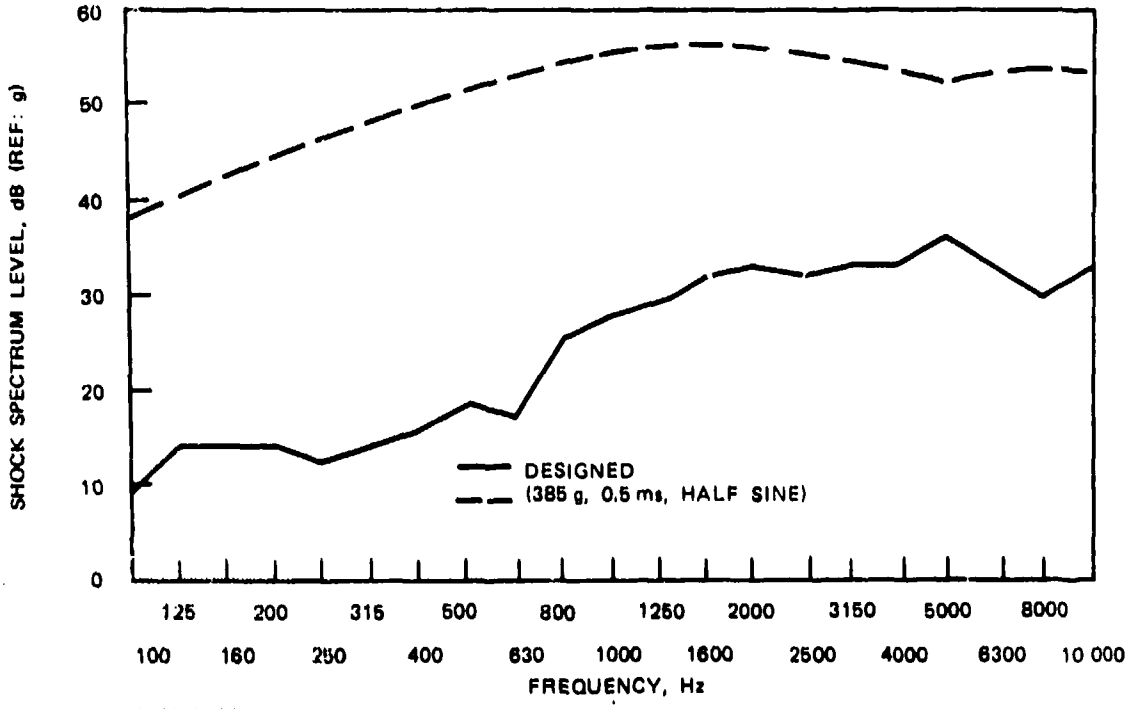

FIGURE 23. Comparison of Q = 10 Shock Spectrum Levels and Design Criterion for Seeker.

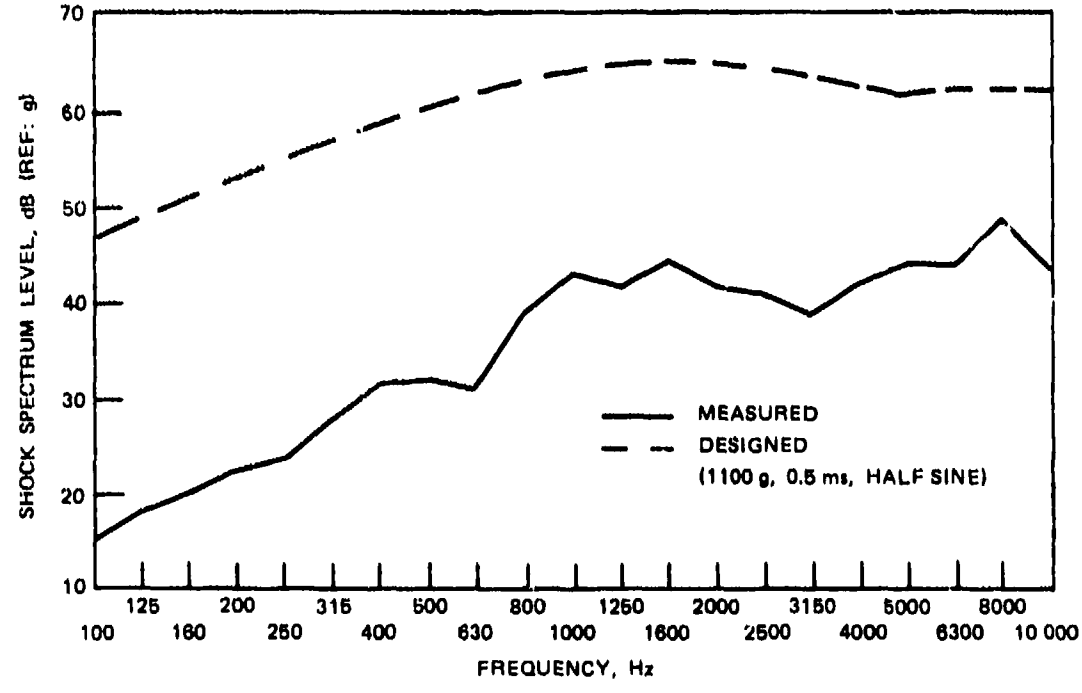

FIGURE 24. Comparison of Q = 10 Shock Spectrum Levels and Design Criterion for Proximity Fuze.

COMPARISONS BASED UPON ENERGY SPECTRA

Figure 25 compares the energy spectrum for the design criteria to the measured energy spectrum of the missile response at the seeker. As before, the measured energy spectrum represents the maximum spectral value computed in all directions at that location, independently for each 1/3-octave band, during ejection from the Aero-7A-1 rack with high-force cartridges. Since the energy spectra for both the design criteria and actual data fall off to insignificant values at the higher frequencies, results are shown for the frequency range up to 2500 Hz only. The energy spectra measured at this location displayed considerable scatter, and the data were heavily smoothed to arrive at the results shown in Figure 25. It is seen, however, that the energy spectrum of the shock response measured on the seeker bulkhead falls surprisingly close to the design requirement at most frequencies. In general, the design requirement appears to be slightly conservative.

Comparing the results in Figure 25 to those previously presented in Figure 23, it is seen that the energy spectrum levels are generally higher relative to the equipment design criterion than the shock spectrum levels at the same equipment location. This observation points out a major deficiency in the use of energy spectra for multiple event data of the type involved in those experiments. Specifically, the missile shock response-time history for any given ejection includes at least three distinct transient events that are rather widely separated in time, as previously detailed in the "Acceleration-Time Histories and Related Parameters" section. The energy spectrum for the entire shock response-time history includes contributions from all of these individual events. Furthermore, the repetition of distinct events with a relatively wide time separation causes a strong low frequency contribution to appear in the overall energy spectrum which is not present in the spectrum of each event taken alone (see Figure 9). These factors are not as influential in a shock spectrum, assuming a reasonable degree of damping. For the case of $Q = 10$, the hypothetical oscillators producing the shock spectrum values will generally decay to near zero response between the separate events, at least at the higher frequencies. This means that the shock spectrum tends to reflect primarily the most severe of the individual transients, which probably constitutes a more realistic measure of damage potential than that provided by the energy spectrum.

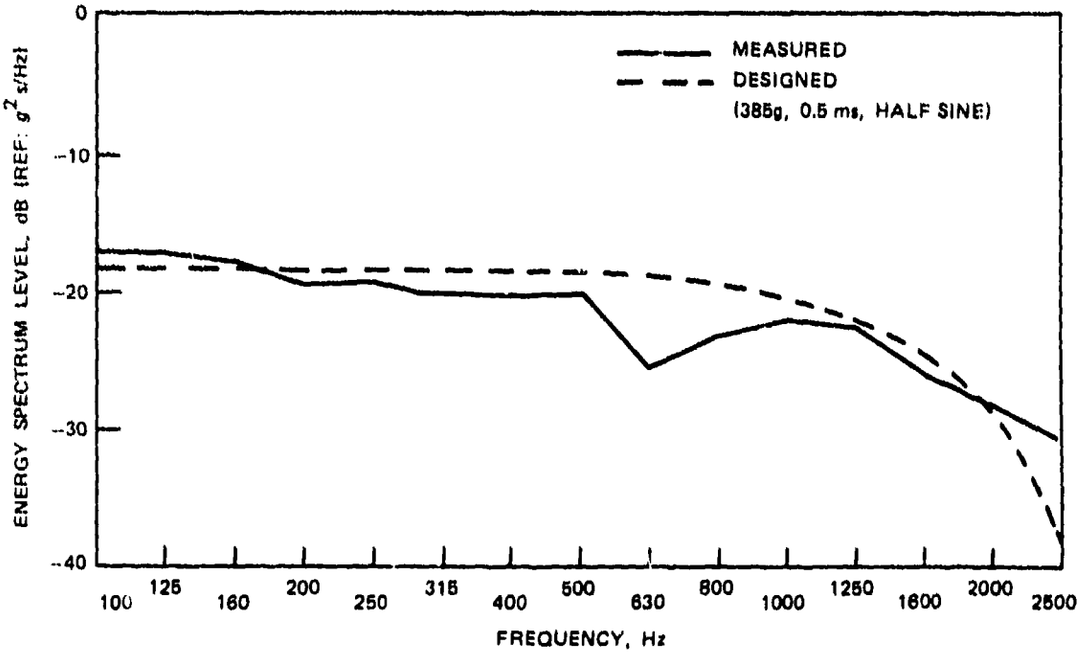

FIGURE 25. Comparison of Energy Spectrum Levels and Design Criterion for Seeker.

CONCLUSIONS

The specific conclusions to be drawn from this study of the Harpoon missile response to simulated launch ejection shock loads may be summarized as follows.

1. The response of the missile is sensitive to the clearance between the ejector foot and the missile. Specifically, the average shock spectra of the acceleration response at frequencies above 800 Hz were up to 6 dB (100%) higher when the clearance was increased from normal (less than 1/16 inch (1.6 mm)) to 1/4 inch (6.4 mm).

2. The acceleration response shock spectrum levels computed for Q = 100 exceed those computed for Q = 10 by about 1 dB at frequencies below 800 Hz and about 4 dB at frequencies above 800 Hz.

3. The shock spectra of the acceleration responses are generally highest along the vertical axis of the missile and lowest in the axial direction. However, the differences among the three orthogonal axes are not significant in the frequency range below 800 Hz. At the higher frequencies, the vertical response is up to 4 dB (60%) higher than the axial response.

4. The response of the missile is about the same for ejections from the MAU-9A/A rack and the Aero-7A-1 rack using similar cartridge combinations.

5. The response of the missile is higher when ejection cartridges of greater force are used. When the nominal force of the ejection cartridges was doubled, the average shock spectrum of the acceleration responses increased by about 4 dB (60%) in the frequency range below 800 Hz. At the higher frequencies, the shock spectrum levels increased by less than 2 dB (25%).

6. The response of the missile falls off dramatically with distance from the ejector foot impact location. For example, the peak acceleration levels at a location only 10 inches (8.3 m) from the ejector foot were about 16% of those measured at the ejector foot location. The lowest levels were measured in the seeker section near the nose of the missile, where the peak acceleration was only 4% of that measured at the ejector foot. In terms of shock spectra, the levels in the seeker section were 20 to 30 dB lower than at the ejector foot location, indicating that the ejection shock is strongly attenuated with distance.

7. In terms of shock spectrum levels, the environmental design criteria for the missile ejection shock loads are generally conservative. At some locations the design criteria exceed the measured response levels by up to 20 dB (10:1).

The above specific conclusions apply rigorously to the Harpoon missile only. Yet most of the conclusions could probably be applied to another missile of similar construction, assuming that differences in key structural parameters are properly taken into account. For example, the flexural hoop mode of the missile shell appears to constitute an important parameter in establishing the response characteristics of the missile as measured by a shock spectrum. Hence, conclusions 1, 2, 3 and 6 might be assumed in the preliminary design of a new missile by scaling the shock spectra frequencies with the ratio of the estimated frequency of the first flexural hoop mode of the new missile, relative to the Harpoon missile. This scaling can generally be accomplished using the simple parameter t/R^2 where t is the missile shell thickness and R is the missile radius.

Appendix A
REVIEW OF TECHNIQUES FOR EVALUATING TRANSIENT DATA

BACKGROUND

Simple transients involving only one or a few oscillations that are basically deterministic in character (that is, highly repetitious in detail from one sample record to the next for a repeated experiment) can sometimes be described adequately for desired applications solely in terms of a response-time history, or some pertinent property of the history such as a peak value and duration. For these cases the transient can often be approximated by some classical waveform (for example, an N wave for sonic booms) which can then be used to evaluate the response of any structure of interest, or to simulate the transient for testing purposes.

For transients that are more complex or stochastic in character, a response-time history by itself is generally of only limited value. Properties of a given history, such as the peak value and duration, may vary significantly from one sample record to the next for a repeated experiment, and also may not fully define the dynamic characteristics of the transient. Examples here include many transients originating from ordnance explosions, particularly when the transients represent the response of some point on a complex structure. The acceleration response data measured at various points on the Harpoon missile structure during aircraft ejection fall into this category. In such cases it is generally more convenient to evaluate the transient for both structural analysis and simulation purposes in terms of some statistically pertinent spectral parameter, rather than in terms of direct response-time histories.

The classical random noise theory provides several techniques that are applicable to the analysis of general nonstationary stochastic phenomena, including complex mechanical shocks. In particular, such data can be analyzed in terms of either a generalized power spectrum or an instantaneous power spectrum, if an ensemble of sample records from repeated trials of an experiment is available.[2] The generalized power spectral density function provides a spectral description in a double frequency plane; the instantaneous power spectral density function yields a time-dependent spectrum. The advantage of such descriptions is that they provide rigorous analytical input-output relationships for structural analysis problems. Their principal disadvantage is that they require considerable data from repeated trials of the experiment of interest that can be voluminous, and the resulting spectra are difficult to interpret in qualitative terms.

For the case of transients that have a clearly defined beginning and end, an overall spectral description for the entire transient event, as opposed to a time-dependent spectral description, is usually satisfactory from the applications viewpoint, and much easier to measure and interpret. Two such overall spectral descriptions in common use are the energy spectrum and the shock response spectrum.

ENERGY SPECTRA

Consider a transient time history record $x(t)$ which is nonzero only over a finite time interval $t_0 \leq t \leq t_0 + T$. For the problem at hand, $x(t)$ would be an acceleration measurement, although it might be any measurement parameter of interest. This history can be transformed into the frequency domain via its Fourier transform given by

[2] J. S. Bendat, and A. G. Piersol. *Random Data: Analysis and Measurement Procedures*. New York, Wiley-Interscience, 1971. Pp. 360-62.

$$X(f) = \int_{-\infty}^{\infty} x(t)e^{-j2\pi ft}dt = X_R(f) - jX_I(f) \tag{A-1}$$

where

$$X_R(f) = \int_{t_o}^{t_o+T} x(t)\cos 2\pi ft \; dt \tag{A-1a}$$

$$X_I(f) = \int_{t_o}^{t_o+T} x(t)\sin 2\pi ft \; dt \tag{A-1b}$$

so long as $x(t) = 0$ except for $t_o \leq t \leq t_o + T$. The real part of the Fourier transform, $X_R(f)$, defines the coincident portion of the Fourier spectrum while the imaginary part, $X_I(f)$, gives the quadrature portion. The Fourier transform may also be expressed in complex polar notation by

$$X(f) = |X(f)|\, e^{-j\theta(f)} \tag{A-2}$$

where

$$|X(f)| = \left[X_R^2(f) + X_I^2(f)\right]^{1/2} \tag{A-2a}$$

$$\theta(f) = \tan^{-1}\left[X_I(f)/X_R(f)\right] \tag{A-2b}$$

The absolute value of the transform, $|X(f)|$ yields its magnitude and the argument, $\theta(f)$, defines an associated phase angle.

The Fourier transform given by Equations (A-1) and (A-2) provides a convenient and analytically useful spectral description of a transient, but one that is uniquely related to the exact transient history; i.e., $X(f)$ defines one and only one $x(t)$. Hence, the use of an $X(f)$ computed from the history produced by a single trial of an experiment introduces the same problems associated with the use of $x(t)$; specifically, $X(f)$ will vary from trial to trial of a given experiment if the transient is stochastic in character. However, for many mechanical, shock-type transients, the stochastic character of the transient is more apparent in the argument of the Fourier transform than in its magnitude. To be specific, if an experiment producing a stochastic transient history is repeated many times, the spectral energy of the resulting histories, as given by

$$E_X(f) = |X(f)|^2 = X_R^2(f) + X_I^2(f) \tag{A-3}$$

will often be quite consistent from one sample record to the next, even though the associated phase factor, $\theta(f)$, might vary dramatically. For many applications, the energy spectrum alone will provide adequate information.

The energy spectrum $E(f)$ for a transient is analogous to the power spectrum commonly used to describe the spectral content of stationary random vibrations, and is interpreted and applied in the

same way. When given two statistically independent transients, $x(t)$ and $y(t)$, their energy spectra are additive, i.e.,

$$E_{x+y}(f) = E_x(f) + E_y(f) \tag{A-4}$$

Furthermore, if $y(t)$ if the response to an excitation $x(t)$, then

$$E_y(f) = |H(f)|^2 E_x(f) \tag{A-5}$$

where $H(f)$ is the frequency response function of the system between $x(t)$ and $y(t)$. The energy spectrum $E(f)$ is computed in the same way as the power spectrum, except that a division by the analysis time T is not required and the error problems are slightly different. Hence, conventional power spectrum computational procedures and analyzers can be used to calculate $E(f)$ with only minor changes in the calibration procedure.

The primary advantage of the energy spectrum as a descriptor of mechanical shock environments lies in the implications of Equations (A-4) and (A-5). The principal disadvantage is that the energy spectrum, like the power spectrum of a stationary vibration, does not yield direct interpretations of the damage potential of the transient. Additional information and analytical effort are needed to translate such spectral representations into a damage potential.[3] On the other hand, the energy spectrum does provide a convenient criterion for simulating shocks in the laboratory.

SHOCK RESPONSE SPECTRA

Unlike the energy spectrum, which evolves basically from analytical concepts, the shock response spectrum is an engineering function designed to describe transient events in terms directly related to the damaging potential of such events. The concept of the shock spectrum is thoroughly developed in the engineering literature, and has been widely applied to aerospace mechanical shock problems.[4,5] Furthermore, it is commonly used as a criterion for the mechanical shock testing of aerospace hardware.[6]

In general terms, the shock spectrum of an acceleration transient $x(t)$ is defined as the maximum response of a damped spring-mounted mass when $x(t)$ is applied at its foundation. The response is calculated as a function of the natural frequency of the spring mass system. The resulting spectrum of peak response values may be defined in terms of any response parameter of interest. In practice, relative displacement (proportional to stress) is widely used to describe mechanical shocks for load-carrying structures, whereas absolute acceleration is more common for equipment packages. In some cases the shock spectrum is presented in terms of psuedo-velocity parameter, which is defined as $2\pi f S_d(f)$, where $S_d(f)$ is the relative displacement shock spectrum. In any case, the interpretation of the shock spectrum is as follows: Given any system of interest that behaves like a

[3]S. H. Crandall, and W. D. Mark. *Random Vibration in Mechanical Systems*. New York, Academic Press, 1963. Pp. 103-25.

[4]S. Rubin, "Concepts Shock Data Analysis," *Shock and Vibration Handbook*, ed. by C. M. Harris and C. E. Crede. New York, McGraw Hill, 1961. Chap. 23.

[5]DOD Shock and Vibration Information Center. *Principles and Techniques of Shock Data Analysis*, by R. D. Kelly and G. Richman. Washington, D.C., SVIC, 1969. (SVM-5.) Pp. 61-79.

[6]Goddard Space Flight Center. *General Environmental Test Specifications for Spacecraft and Components*. Beltsville, Md., GSFC, 1969. (S-320-G-1.)

linear oscillator, the shock spectrum directly defines the maximum strain, acceleration, or other failure-related parameter value that the system will experience when subjected to the shock, depending only upon its natural frequency and damping.

One may define and measure more specific types of shock spectra depending upon the application. For example, the maximum response of the hypothetical spring mass system in the positive and negative directions may be separated to arrive at the positive shock spectrum and the negative shock spectrum. Furthermore, the maximum response that occurs during the application of the input transient might be distinguished from the maximum response after the input transient has terminated. The frequency plot of maximum response during the transient is called the primary shock spectrum, and the plot of maximum response after the transient is called the residual shock spectrum. The plot of maximum values independent of their direction or time of occurrence is often called the maximax shock spectrum.

A key parameter in any type of shock spectrum presentation is the damping ratio assumed for the hypothetical spring mass system. If the shock spectrum concept is to be meaningful, this damping ratio obviously should be similar to the actual damping of the physical system which must survive the shock. For single pulse (nonoscillatory) transients, the damping ratio does not have a major impact on the resulting shock spectrum. However, for oscillatory transients, the damping ratio has a profound impact on the resulting spectrum.

The principal advantage of the shock spectrum lies in its direct interpretation in terms of a failure criterion. It also provides a convenient criterion for simulating shocks in the laboratory. Its disadvantages are associated with the critical assumptions involved in its application, in particular, the assumption that the system of interest will behave as a linear spring mass system with a known damping ratio. For the case of transients that are oscillatory in character, the assumed damping ratio is particularly critical. The Harpoon missile ejection shock data of interest in this study are of the type where the assumed damping ratio significantly influences the resulting shock spectra calculations. To help circumvent this problem, the shock spectra were computed using two damping ratios, 5% (Q = 10) and 0.5% (Q = 100). It is believed that these two damping ratios will bound the actual damping of most structural members and components of the missile.

COMPARISONS OF ENERGY AND SHOCK SPECTRA

Energy and shock spectra evolve from totally different concepts and are generally interpreted in different ways. However, the two functions do have one direct analytical relationship. Specifically, given an acceleration time history $x(t)$, the residual shock spectrum of acceleration values computed using zero damping is given by

$$S_x(f)_r = 2\pi f \left[E_x(f) \right]^{1/2} \tag{A-6}$$

where $E_x(f)$ is the energy spectrum of $x(t)$.[4] It is important to note the frequency dependence in Equation (A-6); i.e., shock spectrum values increase relative to the energy spectrum values as frequency increases. Although this relationship is rigorously correct only for undamped residual shock spectra, there is a tendency in practice for damped maximax shock spectra to display a similar frequency dependence. The reason for this is obvious if one remembers that the shock spectrum is related to the response of a linear oscillator excited by the transient. The half-power point bandwidth of a linear oscillator with fixed damping factor Q is approximately proportional to its natural frequency, f_n, i.e., $B \simeq f_n/Q$. Hence, the bandwidth of the energy that the oscillator will respond to increases with frequency. Given an acceleration transient with an energy spectrum $E_x(f)$, it follows that the acceleration shock spectrum $S_x(f)$ will increase relative to $E_x(f)$ as f increases.

INITIAL DISTRIBUTION

27 Naval Air Systems Command
- AIR-03P (1)
- AIR-30212 (2)
- AIR-320 (1)
- AIR-330D (1)
- AIR-350 (1)
- AIR-5108C (1)
- AIR-5108C1 (1)
- AIR-5109B (1)
- AIR-5109B1 (1)
- AIR-5109E (5)
- AIR-5205 (1)
- AIR-53232 (1)
- AIR-53321 (1)
- AIR-5336 (1)
- AIR-5351 (1)
- AIR-5366 (1)
- AIR-53662 (1)
- AIR-53663 (1)
- AIR-53664 (1)
- AIR-954 (2)
- PMA-258 (1)

2 Chief of Naval Operations
- OP-703 (1)
- OP-722C (1)

1 Chief of Naval Material (MAT-0325B)

6 Naval Sea Systems Command
- SEA-0331 (1)
- SEA-0332 (1)
- SEA-09G32 (2)
- SEA-55211B (1)
- SEA-93 (1)

3 Naval Air Development Center, Johnsville
- Code AEHE, F. Smith (1)
- Code AM, J. Seidel (1)
- Technical Library (1)

2 Naval Air Engineering Center, Lakehurst (WESCO, C. R. Osmanski)

2 Naval Avionics Facility, Indianapolis
- Code ESS, H. Stone (1)
- Technical Library (1)

3 Naval Ordnance Station, Indian Head
- Code 3012A1, B. Boudreaux (1)
- Code REBO (1)
- Technical Library (1)

2 Naval Postgraduate School, Monterey
- R. E. Ball (1)

L.V. Schmidt (1)
1 Naval Research Laboratory (Technical Library)
1 Naval Ship Missile Systems Engineering Station, Port Hueneme
4 Naval Surface Weapons Center, Dahlgren Laboratory, Dahlgren
Code FVR, R. Hudson (1)
Code TI, J. E. Hurtt (1)
Code WXA, S. H. McElroy (1)
Technical Library (1)
3 Naval Surface Weapons Center, White Oak
Jack Gott (1)
Vic Yarow (1)
Technical Library (1)
1 Naval Undersea Center, San Diego
2 Naval Weapons Support Center, Crane
Code RD (1)
Cal Austin (1)
9 Pacific Missile Test Center, Point Mugu
Code 5330 (1)
Code 5333, C. V. Ryden (1)
Code 5334, Bob Cannon (1)
Code 5700, H. Harrison (1)
A. A. Anderson (1)
F. J. Brennan (1)
Technical Library (1)
2 Office Chief of Research and Development
Col. A. Quinnelly (1)
Technical Library (1)
2 Army Materiel Development & Readiness Command
AMCRD-TV, Navakin (1)
Technical Library (1)
1 Aberdeen Proving Ground (Technical Library)
4 Army Engineer Topographic Laboratories, Fort Belvoir
GS-EC, Brierly (3)
Technical Library (1)
2 Frankford Arsenal
K-3400, D. Askin (1)
Technical Library (1)
1 Harry Diamond Laboratories (Technical Library)
1 Picatinny Arsenal (Technical Library)
1 Headquarters, U. S. Air Force (Debuty Chief of Staff, Research and Development)
1 Air Force Armament Laboratory, Eglin Air Force Base
5 Air Force Rocket Propulsion Laboratory, Edwards Air Force Base
Plans and Program Office (1)
RPMCP (1)
L. Meyer (1)
Technical Library (1)
2 Armament Development and Test Center, Eglin Air Force Base
R. Greene (1)
Technical Library (1)

2 Directorate of Armament Development, Eglin Air Force Base
  Technical Library (1)
3 Wright-Patterson Air Force Base
  AFAL, AFSC (1)
  Charles Thomas (1)
  William Savage (1)
12 Defense Documentation Center
2 Applied Physics Laboratory, JHU, Laurel, MD
  Bill Caywood (1)
1 Bird Engineering Research Associate, Inc., Vienna, VA
1 Convair Division of General Dynamics, San Diego, CA (R. G. Huntington)
4 General Dynamics Corporation, Pomona Division, Pomona, CA
  Code 6-42, H. B. Godwin (1)
  Code 8-101, R. J. Carey (1)
  D. Underhill (1)
  Technical Library (1)
1 Honeywell, Inc., Systems and Reasearch Division, Minneapolis, MN (J. D. Brennan)
1 Hughes Aircraft Company, Canoga Park, CA (R. J. Oedy)
1 Lockheed-California Company, Burbank, CA (Code 01-10, W. Hawkins)
4 Lockheed Propulsion Company, Redlands, CA
  C. J. Barr (1)
  W. A. Stevenson (1)
  Engineering Research, John H. Bonin (1)
  Technical Library (1)
11 McDonnell Douglas Corporation, St. Louis, MO
  J. H. Bell (9)
  J. L. Gubser (1)
  Technical Library (1)
2 Martin Company, Denver, CO
  F. A. Thompson (1)
  Technical Library (1)
1 Raytheon Company, Waltham, MA (D. H. Sanders)
2 Rocketdyne, McGregor, TX
  Sparrow/Shrike Project Manager (1)
  Technical Library (1)
2 Sandia Corporation, Albuquerque, NM
  J. Foley (1)
  Technical Library (1)
1 Sandia Corporation, Livermore, CA (Technical Library)
2 Teledyne, CAE, Toledo, OH
  Harpoon Office (1)
  Technical Library (1)
1 Texas Instruments, Inc., Dallas, TX (Missile & Ordnance Division, J. E. Tepera)
3 The Martin Company, Orlando, FL
  Code 143, J. A. Roy (1)
  P. G. Hahn (1)
  Technical Library (1)
1 Thiokol Chemical Corporation, Wasatch Division, Brigham City, UT (R. Brown)
2 Value Engineering Company, Alexandria, VA
  John Toomey (1)
  Technical Library (1)